Available online at www.sciencedirect.com
SCIENCE DIRECT®
Journal of Sound and Vibration 287 (2005) 177–201
JOURNAL OF SOUND AND VIBRATION
www.elsevier.com/locate/jsvi

Magneto-thermo-elastokinetics of geometrically nonlinear laminated composite plates. Part 2: vibration and wave propagation

Zhanming Qin[a], Davresh Hasanyan[a], Liviu Librescu[a,*], Damodar R. Ambur[b]

[a]*Department of Engineering Science and Mechanics, Virginia Polytechnic Institute and State University, Mail Code (0219), 219 Norris Hall, Blacksburg, VA 24061-0219, USA*
[b]*Structures Division, NASA Glenn Research Center, Cleveland, OH 44135, USA*

Received 25 February 2004; received in revised form 5 October 2004; accepted 28 October 2004
Available online 16 February 2005

Abstract

In Part 1 of this paper, the governing equations of geometrically nonlinear, anisotropic composite plates incorporating magneto-thermo-elastic effects have been derived. In order to gain insight into the implications of a number of geometrical and physical features of the system, three special cases are investigated: (i) free vibration of a plate strip immersed in a transversal magnetic field; (ii) free vibration of the plate strip immersed in an axial magnetic field; (iii) magneto-elastic wave propagations of an infinite plate. Within each of these cases, a prescribed uniform thermal field is considered. Special coupling characteristics between the magnetic and elastic fields are put into evidence. Extensive numerical investigations are conducted and pertinent conclusions which highlight the various effects induced by the magneto-elastic couplings and the finite electroconductivity, are outlined.

1. Introduction

An encompassing magneto-thermo-elastic model of laminated composite, finitely electro-conductive plates has been developed in Part 1. This model incorporates the applied magnetic and

*Corresponding author. Tel.: +1 540 231 4935; fax: +1 540 231 4574.
E-mail address: librescu@vt.edu (L. Librescu).

0022-460X/$ - see front matter © 2004 Elsevier Ltd. All rights reserved.
doi:10.1016/j.jsv.2004.10.053

Nomenclature

$\hat{B}^0_{01}$	non-dimensional axial magnetic field intensity, $\sqrt{2h^3\bar{g}_{11}}B^0_{01}/(I_2\omega_0)$
$\hat{B}^0_{03}$	non-dimensional transversal magnetic field intensity, $(\sqrt{3g_0h}/\sqrt[4]{\rho_0E_0})B^0_{03}$
E_0	reference Young's modulus
g_0	reference electroconductivity
$2h$	thickness of the plate/strip
J	$\sqrt{-1}$
$\bar{k}$	dimensional wave number, see Eq. (43)
$2\ell_1$	width of the plate strip
N_L	number of the constituent layers
N_m	number of shape functions used in spatial discretization
z_k	x_3 coordinate of the lower surface of the kth constituent layer
$[\theta_{n_1}/\theta_{n_2}/\cdots]$	sequence of lamination
$\hat{\Theta}$	dimensionless temperature parameter, $\Theta\alpha_0\ell_1^2/h^2$
$\hat{\Theta}^\star$	dimensionless buckling temperature parameter
$\hat{\Theta}^{\mathrm{od}}$	dimensionless temperature parameter which separates the regions of damped/over-damped vibrations
κ	dimensionless parameter, $\bar{k}h$ (see Eq. (44a))
μ_0	magnetic permeability of the vacuum
ρ_0	mass density (per volume) of the plate strip
τ	dimensionless time, see Eq. (12b)
χ	transversal component of the perturbed magnetic field
$\bar{\Xi}$	$\bar{g}_{11}\bar{g}_{22}-\bar{g}_{12}^2$
$\hat{\omega}_\perp$	dimensionless frequency of the flexural wave
$\hat{\omega}_\parallel$	dimensionless frequency of the in-plane wave
$\wp$	incident angle of the magneto-elastic wave
EGM	the Extended Galerkin's Method
TS	the transversely shearable plate model
NTS	the unshearable plate model
$(\dot{(\cdot)},\ddot{(\cdot)}) \equiv (\partial(\cdot)/\partial t, \partial^2(\cdot)/\partial^2 t)$	
$(\dot{(\cdot)},\ddot{(\cdot)}) \equiv (\partial(\cdot)/\partial \tau, \partial^2(\cdot)/\partial \tau^2)$	
$((\cdot)_{,1},(\cdot)_{,2}) \equiv (\partial(\cdot)/\partial x_1, \partial(\cdot)/\partial x_2)$	
$(\hat{(\cdot)}',\hat{(\cdot)}'') \equiv (\partial\hat{(\cdot)}/\partial\xi_1, \partial^2\hat{(\cdot)}/\partial\xi_1^2)$	

the in-plane electric current, both considered to feature arbitrary directions. Such generalities contribute to the full coupling among the magnetic, thermal and elastic fields. Furthermore, the interaction between the induced magnetic field inside and outside the plate is governed by a singular integral equation, whose solution is highly challenging even through a numerical procedure (see, e.g., Ref. [2, pp. 228–229]).

In order to get insight into the magneto-thermo-elastic behavior of laminated composite plates with finite electroconductivity, we will restrict our attention to some special cases of the magnetic and electric current fields: the magnetic field is considered to be either transversal or longitudinal, while the applied electric current field is restricted to be zero. Furthermore, the geometry of the plate will be restricted to either a plate strip or an infinite plate. It is further assumed that the plate strip is subjected to a uniformly distributed temperature change, i.e., $\Theta_0 = \text{const.}$ and $\Theta_1 = 0$.

The special cases to be investigated in this article include:

- free vibrational behavior of a plate strip in a transversal magnetic field;
- free vibrational behavior of a plate strip in an axial magnetic field;

- magneto-elastic wave propagation of an infinite plate in a transversal magnetic field;

The influence of the transverse shear, lay-up scheme, and of the finite electroconductivity on the free vibration and the dispersion relations will be specifically addressed.

2. Case I: free vibration of a plate strip in a transversal magnetic field

2.1. Governing equations

The case of a plate strip, infinite in the x_2 direction is considered. For this case, $B_{01} = B_{02} = 0, B_{03} \neq 0$, and the whole set of the 10 basic unknowns v_i $(i = 1, 2, 3), \beta_\alpha$ $(\alpha = 1, 2), \chi, \varphi$ and ψ become functions of (x_1, t) only. Moreover, due to its definition, γ_1 becomes zero as well. The Lorentz forces f_i (see Part 1 for its expressions) can be represented as

$$f_1 = j_2 B_{03}^0, \quad f_2 = -j_1 B_{03}^0, \quad f_3 = 0, \tag{1a–c}$$

in which the induced electric current components j_1 and j_2 are defined as

$$j_1 = g_{11}^{(i)}[\varphi + \dot{v}_2 B_{03}^0] + g_{12}^{(i)}[\psi - \dot{v}_1 B_{03}^0] + x_3[g_{11}^{(i)}\dot{\beta}_2 - g_{12}^{(i)}\dot{\beta}_1]B_{03}^0, \tag{2a}$$

$$j_2 = g_{12}^{(i)}[\varphi + \dot{v}_2 B_{03}^0] + g_{22}^{(i)}[\psi - \dot{v}_1 B_{03}^0] + x_3[g_{12}^{(i)}\dot{\beta}_2 - g_{22}^{(i)}\dot{\beta}_1]B_{03}^0. \tag{2b}$$

In Eqs. (2a, b), $x_3 \in [z_i, z_{i+1})$. As a result, the generalized forces of electrodynamical origin become:

$$\int_{-h}^{h} f_1 \, \mathrm{d}x_3 = (2h)[\bar{g}_{12}(\varphi + \dot{v}_2 B_{03}^0) + \bar{g}_{22}(\psi - \dot{v}_1 B_{03}^0)]B_{03}^0, \tag{3a}$$

$$\int_{-h}^{h} f_2 \, \mathrm{d}x_3 = -(2h)[\bar{g}_{11}(\varphi + \dot{v}_2 B_{03}^0) + \bar{g}_{12}(\psi - \dot{v}_1 B_{03}^0)]B_{03}^0, \tag{3b}$$

$$\int_{-h}^{h} x_3 f_1 \, \mathrm{d}x_3 = [C_{12}^g \dot{\beta}_2 - C_{22}^g \dot{\beta}_1](B_{03}^0)^2, \tag{3c}$$

$$\int_{-h}^{h} x_3 f_2 \, \mathrm{d}x_3 = [-C_{11}^g \dot{\beta}_2 + C_{12}^g \dot{\beta}_1](B_{03}^0)^2, \tag{3d}$$

where

$$C_{\alpha\beta}^g \equiv 2h\mathscr{M}_2[g_{\alpha\beta}], \quad \bar{g}_{\alpha\beta} \equiv \mathscr{M}_0[g_{\alpha\beta}], \quad (\alpha, \beta) = 1, 2, \tag{4a, b}$$

and $z_k \equiv -h + (k-1)2h/N_L, (k = \overline{1, N_L})$. It is recalled that the operators $\mathscr{M}_0$ and $\mathscr{M}_2$ are defined in Appendix C, Part 1.

The diffusion equation which governs the induced magnetic field χ now reduces to

$$\bar{g}_{11}\chi_{,11} - \bar{\Xi}\mu\dot{\chi} = \bar{g}_{11}\frac{1}{2h}\gamma_{2,1} + \bar{\Xi}\dot{v}_{1,1}B_{03}^0. \tag{5}$$

The quantity γ_2 in Eq. (5) should be determined from Eq. (42) and the boundary condition (40b) of Part 1.

The exact solution of γ_2 is [3]

$$\gamma_2(x_1,t) = -\frac{2}{\pi}\frac{1}{\sqrt{\ell_1^2 - x_1^2}}\int_{-\ell_1}^{\ell_1}\frac{\sqrt{\ell_1^2 - s_1^2}}{s_1 - x_1}\,\chi(s_1,t)\,\mathrm{d}s_1. \tag{6}$$

Substitution of Eq. (6) into Eq. (5) yields the following differential-singular integral equation governing χ:

$$\begin{aligned}&\bar{g}_{11}\chi_{,11} - \bar{\Xi}\mu\dot{\chi} + \bar{g}_{11}\frac{x_1}{\pi h\sqrt{[\ell_1^2 - x_1^2]^3}}\int_{-\ell_1}^{\ell_1}\frac{\sqrt{\ell_1^2 - s_1^2}}{s_1 - x_1}\chi(s_1,t)\,\mathrm{d}s_1\\ &+ \bar{g}_{11}\frac{1}{\pi h\sqrt{\ell_1^2 - x_1^2}}\frac{\partial}{\partial x_1}\int_{-\ell_1}^{\ell_1}\frac{\sqrt{\ell_1^2 - s_1^2}}{s_1 - x_1}\,\chi(s_1,t)\,\mathrm{d}s_1 = \bar{\Xi}\dot{v}_{1,1}B_{03}^0.\end{aligned} \tag{7}$$

It is worth noting that the full solution of χ depends only on v_1.

The solutions of φ and ψ reduce to

$$\left\{\begin{array}{c}\varphi\\ \psi\end{array}\right\} = \frac{1}{\bar{\Xi}}\left\{\begin{array}{l}\bar{g}_{22}[-\bar{g}_{11}\dot{v}_2 + \bar{g}_{12}\dot{v}_1]B_{03}^0 + \bar{g}_{12}\left[\chi_{,1} - \dfrac{\gamma_2}{2h} + (\bar{g}_{12}\dot{v}_2 - \bar{g}_{22}\dot{v}_1)B_{03}^0\right]\\ \bar{g}_{12}[\bar{g}_{11}\dot{v}_2 - \bar{g}_{12}\dot{v}_1]B_{03}^0 + \bar{g}_{11}\left[-\chi_{,1} + \dfrac{\gamma_2}{2h} - (\bar{g}_{12} - \bar{g}_{22}\dot{v}_1)B_{03}^0\right]\end{array}\right\}. \tag{8}$$

Within the linear theory of shearable plates, the corresponding governing equations can be simplified as

$$\delta v_1 : A_{11}v_{1,11} + A_{16}v_{2,11} - I_0\ddot{v}_1 + (2h)[\bar{g}_{12}(\varphi + \dot{v}_2B_{03}^0) + \bar{g}_{22}(\psi - \dot{v}_1B_{03}^0)]B_{03}^0 = 0, \tag{9a}$$

$$\delta v_2 : A_{16}v_{1,11} + A_{66}v_{2,11} - I_0\ddot{v}_2 - (2h)[\bar{g}_{11}(\varphi + \dot{v}_2B_{03}^0) - \bar{g}_{12}(\psi - \dot{v}_1B_{03}^0)]B_{03}^0 = 0, \tag{9b}$$

$$\delta v_3 : A_{45}\beta_{2,11} + A_{55}(\beta_{1,1} + v_{3,11}) - A_{11}^{\alpha}\Theta v_{3,11} - I_0\ddot{v}_3 = 0, \tag{9c}$$

$$\delta\beta_1 : D_{11}\beta_{1,11} + D_{16}\beta_{2,11} - A_{45}\beta_2 - A_{55}(\beta_1 + v_{3,1}) - I_2\ddot{\beta}_1 + (B_{03}^0)^2C_{12}^g\dot{\beta}_2 - (B_{03}^0)^2C_{22}^g\dot{\beta}_1 = 0, \tag{9d}$$

$$\delta\beta_2 : D_{16}\beta_{1,11} + D_{66}\beta_{2,11} - A_{44}\beta_2 - A_{45}(\beta_1 + v_{3,1}) - I_2\ddot{\beta}_2 - (B_{03}^0)^2C_{11}^g\dot{\beta}_2 + (B_{03}^0)^2C_{12}^g\dot{\beta}_1 = 0. \tag{9e}$$

Herein, A_{11}^{α} is defined as

$$A_{11}^{\alpha} \equiv \int_{-h}^{h}(A_{11}\alpha_{11} + A_{12}\alpha_{22} + A_{16}\alpha_{12})\,\mathrm{d}x_3. \tag{10}$$

Since χ depends on v_1, see Eqs. (5) and (6), from Eq. (8) it can be seen that φ and ψ depend only on v_1 and v_2. Therefore, from Eqs. (9a–e), it is concluded that the in-plane magneto-elastic

vibrations associated with v_1 and v_2 are completely decoupled from the flexural ones associated with v_3, β_1 and β_2. In the following, the study will be restricted to flexural vibrations.

If transverse shear effects are further discarded, implying $\beta_1 \to -v_{3,1}$ and $\beta_2 \to -v_{3,2} = 0$, then the flexural vibration is entirely governed by v_3. As a result, the governing equations reduce to

$$D_{11}v_{3,1111} + \underbrace{(A^{\alpha}_{11}\Theta)v_{3,11}}_{a} - \underbrace{(B^0_{03})^2 C^g_{22}\dot{v}_{3,11}}_{b} - \underbrace{I_2\ddot{v}_{3,11}}_{c} + I_0\ddot{v}_3 = 0. \tag{11}$$

In Eq. (11), it is noted that the term labelled by "a" can be viewed as corresponding to a compressive edge load that can yield buckling; the term indicated by "b" provides damping; while the term labelled by "c" is associated with the rotary inertia. It is further remarked that in the case of a single-layered plate (i.e., $N_L = 1$), $C^g_{22} \to 2h^3 g_{22}/3$ and Eq. (11) exactly reduces to the equation used in Ref. [4].

2.2. Flexural vibration analysis of a clamped–clamped plate strip

Using the following non-dimensional parameters:

$$\xi_1 \equiv x_1/\ell_1, \quad \tau \equiv t\sqrt{\frac{D_{11}}{I_0\ell_1^4}}, \quad \hat{v}_3 \equiv v_3/h. \tag{12a–c}$$

Eq. (11) becomes

$$\frac{\partial^4\hat{v}_3}{\partial\xi_1^4} + A^{\alpha}_{11}\Theta\,\frac{\ell_1^2}{D_{11}}\frac{\partial^2\hat{v}_3}{\partial\xi_1^2} - \frac{(B^0_{03})^2 C^g_{22}}{\sqrt{D_{11}I_0}}\frac{\partial^3\hat{v}_3}{\partial\xi_1^2\partial\tau} - \frac{I_2}{I_0\ell_1^2}\frac{\partial^4\hat{v}_3}{\partial\xi_1^2\partial\tau^2} + \frac{\partial^2\hat{v}_3}{\partial\tau^2} = 0. \tag{13}$$

In order to solve Eq. (13), the Extended Galerkin's Method (EGM) will be used. The underlying idea of such method is that the adopted shape functions should only satisfy the geometric boundary conditions, while the natural boundary conditions that may not be satisfied appear as a residual in the functional that should be minimized in the Galerkin sense.

We introduce the spatial discretization:

$$\hat{v}_3 = \hat{\mathbf{\Psi}}(\xi_1)\hat{\mathbf{q}}(\tau), \tag{14}$$

in which, the shape function vector $\hat{\mathbf{q}}(\xi_1)$ needs only fulfill the geometric boundary conditions. Then Eq. (13) reduces to a set of ordinary differential equations:

$$\mathbf{M}_{qq}\ddot{\hat{\mathbf{q}}} + \mathbf{C}_{qq}\dot{\hat{\mathbf{q}}} + \mathbf{K}_{qq}\hat{\mathbf{q}} = 0. \tag{15}$$

In Eq. (15), as well as in the following ones, no summation convention over a repeated index is implied; the entries of the mass, damping and stiffness matrices $\mathbf{M}_{qq}$, $\mathbf{C}_{qq}$, $\mathbf{K}_{qq}$, respectively, are defined in Appendix A. We note that the matrix $\mathbf{C}_{qq}$ is a function of B^0_{03}, while $\mathbf{K}_{qq}$ is a function of Θ. From Eq. (15), the condition for the plate strip to be thermally buckled can be expressed by $\det(\mathbf{K}_{qq}) = 0$.

Further, casting Eq. (15) in the state-space form, we get

$$\begin{Bmatrix} \dot{\hat{\mathbf{q}}} \\ \ddot{\hat{\mathbf{q}}} \end{Bmatrix} = \begin{bmatrix} \mathbf{0} & \mathbf{I} \\ -(\mathbf{M}^{-1}_{qq}\mathbf{K}_{qq}) & -(\mathbf{M}^{-1}_{qq}\mathbf{C}_{qq}) \end{bmatrix} \begin{Bmatrix} \hat{\mathbf{q}} \\ \dot{\hat{\mathbf{q}}} \end{Bmatrix}. \tag{16}$$

Eqs. (14) and (16) are related to the numerical solution of the unshearable plate model. Toward the numerical solution of the transversely shearable model, we start with Eqs. (9c–e) and use the following spatial discretization:

$$\hat{v}_3 = \hat{\mathbf{\Psi}}_v^{\mathrm{T}}(\xi_1)\hat{\mathbf{q}}_v(\tau), \quad \beta_1 = \hat{\mathbf{\Psi}}_{\beta_1}^{\mathrm{T}}(\xi_1)\hat{\mathbf{q}}_{\beta_1}(\tau), \quad \beta_2 = \hat{\mathbf{\Psi}}_{\beta_2}^{\mathrm{T}}(\xi_1)\hat{\mathbf{q}}_{\beta_2}(\tau). \tag{17a–c}$$

As a result, Eqs. (9c–e) can be cast as:

$$\begin{bmatrix} \mathbf{M}_{vv} & \mathbf{0} & \mathbf{0} \\ \mathbf{0} & \mathbf{M}_{\beta_1\beta_1} & \mathbf{0} \\ \mathbf{0} & \mathbf{0} & \mathbf{M}_{\beta_2\beta_2} \end{bmatrix} \begin{Bmatrix} \ddot{\hat{\mathbf{q}}}_v \\ \ddot{\hat{\mathbf{q}}}_{\beta_1} \\ \ddot{\hat{\mathbf{q}}}_{\beta_2} \end{Bmatrix} + \begin{bmatrix} \mathbf{0} & \mathbf{0} & \mathbf{0} \\ \mathbf{0} & \mathbf{C}_{\beta_1\beta_1} & \mathbf{C}_{\beta_1\beta_2} \\ \mathbf{0} & \mathbf{C}_{\beta_2\beta_1} & \mathbf{C}_{\beta_2\beta_2} \end{bmatrix} \begin{Bmatrix} \dot{\hat{\mathbf{q}}}_v \\ \dot{\hat{\mathbf{q}}}_{\beta_1} \\ \dot{\hat{\mathbf{q}}}_{\beta_2} \end{Bmatrix} + \begin{bmatrix} \mathbf{K}_{vv} & \mathbf{K}_{v\beta_1} & \mathbf{K}_{v\beta_2} \\ \mathbf{K}_{\beta_1 v} & \mathbf{K}_{\beta_1\beta_1} & \mathbf{K}_{\beta_1\beta_2} \\ \mathbf{K}_{\beta_2 v} & \mathbf{K}_{\beta_2\beta_1} & \mathbf{K}_{\beta_2\beta_2} \end{bmatrix} \begin{Bmatrix} \hat{\mathbf{q}}_v \\ \hat{\mathbf{q}}_{\beta_1} \\ \hat{\mathbf{q}}_{\beta_2} \end{Bmatrix} = \begin{Bmatrix} \mathbf{0} \\ \mathbf{0} \\ \mathbf{0} \end{Bmatrix}. \tag{18}$$

In Eq. (18), the entries of the submatrices are defined in Appendix A.

For the clamped–clamped plate strip, the shape function vector $\hat{\mathbf{\Psi}}$ in Eq. (14) and $\hat{\mathbf{\Psi}}_v$, $\hat{\mathbf{\Psi}}_{\beta_1}$, $\hat{\mathbf{\Psi}}_{\beta_2}$ in Eq. (17) can be taken as

$$\hat{\mathbf{\Psi}}^{\mathrm{T}} = \{\cos\pi\xi_1 + 1, \cos 2\pi\xi_1 - 1, \ldots, \cos N_m\pi\xi_1 - (-1)^{N_m}\}, \tag{19a}$$

$$\hat{\mathbf{\Psi}}_v^{\mathrm{T}} = \left\{\cos\frac{\pi}{2}\xi_1, \cos\frac{3\pi}{2}\xi_1, \ldots, \cos\frac{(2N_m-1)\pi}{2}\xi_1\right\}, \tag{19b}$$

$$\hat{\mathbf{\Psi}}_{\beta_1}^{\mathrm{T}} = \{\sin\pi\xi_1, \sin 2\pi\xi_1, \ldots, \sin N_m\pi\xi_1\}, \tag{19c}$$

$$\hat{\mathbf{\Psi}}_{\beta_2}^{\mathrm{T}} = \{\sin\pi\xi_1, \sin 2\pi\xi_1, \ldots, \sin N_m\pi\xi_1\}. \tag{19d}$$

We note that the shape functions in Eq. (19c) are taken in such a way that for the unshearable model, β_1 and $\hat{v}_{3,1}$ have the same shape function space representation.

2.3. Characteristics of flexural vibration of the plate strip

As discussed for Eq. (11) and also revealed by Eqs. (15) and (18), the transversal magnetic field B_{03}^0 plays only the role of damping. For the purpose of clarifying the vibrational behavior of the plate strip, the unshearable model will be adopted and the one-term shape function $\hat{\mathbf{\Psi}} = \cos(2.365\xi) + 0.133\cosh(2.365\xi)$, which is the exact first-order eigenmode of a clamped–clamped beam, will be used. Assuming the synchronous solution $\hat{q}(\tau) = \hat{q}^0\exp(\lambda\tau)$, Eq. (15) reduces to

$$m_{qq}\lambda^2 + c_{qq}\lambda + k_{qq} = 0, \tag{20}$$

in which

$$m_{qq} = 3.127\left[1 + \frac{2}{3}\left(\frac{h}{\ell_1}\right)^2\right], \tag{21a}$$

$$c_{qq} = 1.042(B_{03}^0)^2 \frac{\mathscr{M}_2[g_{22}]/(h^2 E_0)}{\{\mathscr{M}_2[\bar{Q}_{11}]/(h^2 E_0)\}^{1/2}}, \tag{21b}$$

$$k_{qq} = 31.851 - 3.127\hat{\Theta}\frac{\sum_{i=1}^{N_L}[\bar{Q}_{11}^{(i)}\alpha_{11}^{(i)} + \bar{Q}_{12}^{(i)}\alpha_{22}^{(i)} + \bar{Q}_{16}^{(i)}\alpha_{16}^{(i)}]/(N_L\alpha_0)}{\mathscr{M}_2[\bar{Q}_{11}]/h^2}. \tag{21c}$$

In Eqs. (21a–c), g_0, α_0 and E_0 are the reference electric conductivity, thermal expansion coefficient and elastic constant, respectively, while the non-dimensional parameters $\hat{B}_{03}^0$ and $\hat{\Theta}$ are defined as

$$\hat{B}_{03}^0 \equiv B_{03}^0\left(\frac{3g_0 h}{\sqrt{\rho_0 E_0}}\right)^{1/2}, \quad \hat{\Theta} \equiv \frac{\Theta\alpha_0\ell_1^2}{h^2}. \tag{22a, b}$$

Based on Eq. (20), one obtains the vibrational behavior that can be summarized as follows (see Fig. 1, and Ref. [4]):

(i) For $k_{qq} = 0$, the thermal buckling occurs. The critical temperature parameter $\hat{\Theta}^\star$ can be represented as

$$\hat{\Theta}^\star \equiv 10.186\frac{\mathscr{M}_2[\bar{Q}_{11}]/h^2}{\sum_{i=1}^{N_L}[\bar{Q}_{11}^{(i)}\alpha_{11}^{(i)} + \bar{Q}_{12}^{(i)}\alpha_{22}^{(i)} + \bar{Q}_{16}^{(i)}\alpha_{16}^{(i)}]/(N_L\alpha_0)}. \tag{23}$$

When $\hat{\Theta} > \hat{\Theta}$, the plate strip is in the state of post-thermal buckling (within the region denoted by $\mathscr{E}_1$ in Fig. 1).

(ii) For $k_{qq} > 0$ and $c_{qq}^2 - 4m_{qq}k_{qq} \geqslant 0$ (or when $\Theta \in [\hat{\Theta}^{\text{od}}, \hat{\Theta}^\star]$), the plate strip experiences overdamped vibration (within the region denoted by $\mathscr{E}_2$), in which $\hat{\Theta}^{\text{od}}$ is the critical overdamped temperature below which damped oscillation occurs and is defined as

$$\hat{\Theta}^{\text{od}} \equiv 10.186\frac{\mathscr{M}_2[\bar{Q}_{11}]/h^2}{\sum_{i=1}^{N_L}[\bar{Q}_{11}^{(i)}\alpha_{11}^{(i)} + \bar{Q}_{12}^{(i)}\alpha_{22}^{(i)} + \bar{Q}_{16}^{(i)}\alpha_{16}^{(i)}]/(N_L\alpha_0)} - \frac{1}{36}\frac{\{\mathscr{M}_2[g_{22}/g_0]/h^2\}^2}{\sum_{i=1}^{N_L}[\bar{Q}_{11}^{(i)}\alpha_{11}^{(i)} + \bar{Q}_{12}^{(i)}\alpha_{22}^{(i)} + \bar{Q}_{16}^{(i)}\alpha_{16}^{(i)}]/(N_L E_0\alpha_0)}(\hat{B}_{03}^0)^4. \tag{24}$$

(iii) For $k_{qq} > 0$ and $c_{qq}^2 - 4m_{qq}k_{qq} < 0$ (or when $\hat{\Theta} < \hat{\Theta}^{\text{od}}$), the plate strip experiences damped oscillation (within the region denoted by $\mathscr{E}_3$). The eigensolution λ in such a case can be

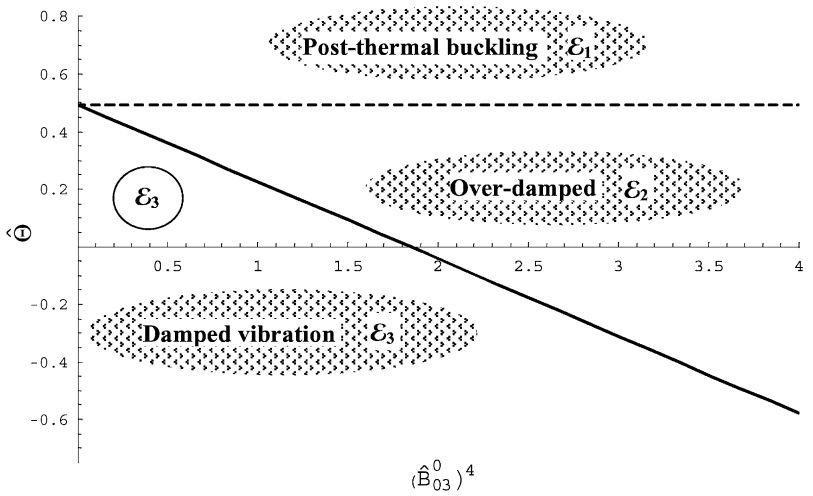

Fig. 1. Qualitative picture of the vibrational behavior of the magneto-thermo-elastic plate strip as influenced by the magnetic and thermal fields (the three regions labelled as $\mathscr{E}_1$, $\mathscr{E}_2$ and $\mathscr{E}_3$ are defined in Section 2.3). The boundary of the thermal buckling is indicated by ------, $\hat{\Theta}^{\star}$; and $\hat{\Theta}^{\mathrm{od}}$ (——) separates the regions $\mathscr{E}_2$ and $\mathscr{E}_3$.

represented as

$$\frac{\lambda}{\omega_0} = -\frac{\sqrt{3}}{6}(\hat{B}^0_{03})^2 \mathscr{M}_2\left[\frac{g_{22}}{g_0}\right] \pm_J \left\{ 30.558 \mathscr{M}_2\left[\frac{\bar{Q}_{11}}{E_0}\right] \Big/ h^2 - 3\hat{\Theta}\left[\sum_{i=1}^{N_L} \frac{\bar{Q}^{(i)}_{11}\alpha^{(i)}_{11} + \bar{Q}^{(i)}_{12}\alpha^{(i)}_{22} + \bar{Q}^{(i)}_{16}\alpha^{(i)}_{12}}{E_0\alpha_0 N_L}\right] - \frac{1}{12}(\hat{B}^0_{03})^4 \left(\mathscr{M}_2\left[\frac{g_{22}}{g_0}\right] \Big/ h^2 \right)^2 \right\}^{1/2}. \tag{25}$$

3. Case II: free vibration of a plate strip in an axial magnetic field

In this case, $B^0_{01} = \text{const.}$, $B^1_{01} = 0$. It is further assumed that $\Theta_0 = 0$. We are still considering the clamped–clamped plate strip. The generalized forces of electrodynamical origin that are displayed in Appendix B of Part 1 reduce to:

$$\int_{-h}^{h} f_2 \, \mathrm{d}x_3 = 0, \tag{26a}$$

$$\int_{-h}^{h} f_3 \, \mathrm{d}x_3 = (-B^0_{01} 2h)[\bar{g}_{12}\varphi + \bar{g}_{22}\psi + \bar{g}_{22}\dot{v}_3 B^0_{01}] = -B^0_{01}[\gamma_2 - 2h\chi_{,1}], \tag{26b}$$

$$\int_{-h}^{h} x_3 f_2 \, \mathrm{d}x_3 = \frac{1}{2} B^0_{01}[C^g_{11}\varphi_{,1} + C^g_{12}(\psi_{,1} + \dot{v}_{3,1} B^0_{01})]. \tag{26c}$$

In Eqs. (26c), $\varphi_{,1}$ and $\psi_{,1}$ can be expressed as

$$\varphi_{,1} = \frac{\bar{g}_{12}}{\bar{g}_{11}}[\mu\dot{\chi} - \dot{v}_{3,1}B^0_{01}], \quad \psi_{,1} = -\mu\dot{\chi}, \tag{27a, b}$$

where χ is governed by the following diffusion equations:

$$\bar{g}_{11}\chi_{,11} - \mu\bar{\Xi}\dot{\chi} = -\bar{\Xi}\dot{v}_{3,1}B^0_{01} + \bar{g}_{11}\frac{1}{2h}\gamma_{2,1}, \tag{28a}$$

$$\gamma_2 = -\frac{2}{\pi}\frac{1}{\sqrt{\ell_1^2 - x_1^2}}\int_{-\ell_1}^{\ell_1}\frac{\sqrt{\ell_1 - s_1^2}}{s_1 - x_1}\chi(s_1, t)\,\mathrm{d}s_1. \tag{28b}$$

From Eqs. (28a, b), it is readily seen that χ and γ_2 are determined by v_3, and from Eqs. (27a, b), it becomes clear that φ and ψ are determined by v_3 only. Therefore, similar to the governing equations in the preceding Case I, the in-plane magneto-elastic vibrations v_α are completely decoupled from the flexural ones described in terms of v_3 and β_α.

In short, the flexural vibrations are governed by

$$\delta v_3 : A_{45}\beta_{2,1} + A_{55}(\beta_{1,1} + v_{3,11}) - I_0\ddot{v}_3 - B^0_{01}(\gamma_2 - 2h\chi_{,1}) = 0, \tag{29a}$$

$$\delta\beta_1 : D_{11}\beta_{1,11} + D_{16}\beta_{2,11} - A_{45}\beta_2 - A_{55}(\beta_1 + v_{3,1}) - I_2\ddot{\beta}_1 = 0, \tag{29b}$$

$$\begin{aligned}\delta\beta_2 : {} & D_{16}\beta_{1,11} + D_{66}\beta_{2,11} - A_{44}\beta_2 - A_{45}(\beta_1 + v_{3,1}) - I_2\ddot{\beta}_2 + \frac{1}{2}B^0_{01}C^g_{11}\varphi_{,1} \\ & + \frac{1}{2}B^0_{01}C^g_{12}(\psi_{,1} + \dot{v}_{3,1}B^0_{01}) = 0.\end{aligned} \tag{29c}$$

where χ and γ_2 are governed by Eqs. (28a,b), while φ and ψ are governed by Eqs. (27a,b), respectively.

It is noted that unlike the transverse magnetic field in Case I, which provides only a damping effect on the motion, in the present Case II, the axial magnetic field modifies both the damping and stiffness coefficients of the plate. In the limiting case of the infinite electroconductivity, from Eq. (28a), $\chi \to H^0_{01}v_{3,1}$. As a result, the damping effect becomes immaterial and the magnetic field only influences the stiffness coefficient.

As to the non-dimensionlization, besides the parameters in Eq. (12), the following ones are further defined:

$$\hat{\chi} \equiv \frac{\bar{g}_{11}}{B^0_{01}\bar{\Xi}\omega_0 h^2}\chi, \quad \hat{\gamma}_2 \equiv \frac{\bar{g}_{11}}{B^0_{01}\bar{\Xi}\omega_0 h^2}\gamma_2, \tag{30a, b}$$

in which $\omega_0 \equiv \sqrt{D_{11}/(\ell_1^4 I_0)}$.

In order to apply the EGM [5,8] for solving the governing equations (29a–c) and (28a,b), spatial discretization is carried out via Eq. (14) and

$$\hat{\chi} = \hat{\mathbf{\Psi}}^{\mathrm{T}}_{\chi}(\xi_1)\hat{\mathbf{q}}_{\chi}(\tau). \tag{31}$$

Similar to the choice of the shape functions of β_1, we select the shape functions of $\hat{\chi}$ in such a way that in the limit of infinite electroconductivity, χ and $v_{3,1}$ have the same shape function space

representation. As a result,

$$\hat{\mathbf{\Psi}}_{\chi}^{\mathrm{T}} = \{\sin \pi\xi_1, \sin 2\pi\xi_1, \ldots, \sin N_m \pi\xi_1\}. \tag{32}$$

Then, the governing equations (29a–c) and (28a) can be cast in the state-space form

$$\begin{Bmatrix} \dot{\hat{\mathbf{q}}}_v \\ \dot{\hat{\mathbf{q}}}_{\beta_1} \\ \dot{\hat{\mathbf{q}}}_{\beta_2} \\ \dot{\hat{\mathbf{q}}}_{\chi} \\ \ddot{\hat{\mathbf{q}}}_v \\ \ddot{\hat{\mathbf{q}}}_{\beta_1} \\ \ddot{\hat{\mathbf{q}}}_{\beta_2} \end{Bmatrix} = \begin{bmatrix} \mathbf{0} & \mathbf{0} & \mathbf{0} & \mathbf{0} & \mathbf{I} & \mathbf{0} & \mathbf{0} \\ \mathbf{0} & \mathbf{0} & \mathbf{0} & \mathbf{0} & \mathbf{0} & \mathbf{I} & \mathbf{0} \\ \mathbf{0} & \mathbf{0} & \mathbf{0} & \mathbf{0} & \mathbf{0} & \mathbf{0} & \mathbf{I} \\ \mathbf{0} & \mathbf{0} & \mathbf{0} & -\mathbf{A}_{\chi}^{-1}\mathbf{B}_{\chi} & \mathbf{A}_{\chi}^{-1}\mathbf{C}_{\chi} & \mathbf{0} & \mathbf{0} \\ -\mathbf{M}_{vv}^{-1}\mathbf{K}_{vv} & -\mathbf{M}_{vv}\mathbf{K}_{v\beta_1} & -\mathbf{M}_{vv}^{-1}\mathbf{K}_{v\beta_2} & -\mathbf{M}_{vv}^{-1}\mathbf{K}_{v\chi} & \mathbf{0} & \mathbf{0} & \mathbf{0} \\ -\mathbf{M}_{\beta_1\beta_1}^{-1}\mathbf{K}_{\beta_1 v} & -\mathbf{M}_{\beta_1\beta_1}^{-1}\mathbf{K}_{\beta_1\beta_1} & -\mathbf{M}_{\beta_1\beta_1}^{-1}\mathbf{K}_{\beta_1\beta_2} & \mathbf{0} & \mathbf{0} & \mathbf{0} & \mathbf{0} \\ -\mathbf{M}_{\beta_2\beta_2}^{-1}\mathbf{K}_{\beta_2 v} & -\mathbf{M}_{\beta_2\beta_2}^{-1}\mathbf{K}_{\beta_2\beta_1} & -\mathbf{M}_{\beta_2\beta_2}^{-1}\mathbf{K}_{\beta_2\beta_2} & -\mathbf{M}_{\beta_2\beta_2}^{-1}\mathbf{K}_{\beta_2\chi} & -\mathbf{M}_{\beta_2\beta_2}^{-1}\mathbf{C}_{\beta_2 v} & \mathbf{0} & \mathbf{0} \end{bmatrix} \begin{Bmatrix} \hat{\mathbf{q}}_v \\ \hat{\mathbf{q}}_{\beta_1} \\ \hat{\mathbf{q}}_{\beta_2} \\ \hat{\mathbf{q}}_{\chi} \\ \dot{\hat{\mathbf{q}}}_v \\ \dot{\hat{\mathbf{q}}}_{\beta_1} \\ \dot{\hat{\mathbf{q}}}_{\beta_2} \end{Bmatrix}. \tag{33}$$

The entries of each submatrix in Eq. (33) are defined in Appendix B. We further note that in order to eliminate the strong singularity present in the last term in Eq. (28a), the following result is used:

$$\int_{-1}^{1} \hat{\mathbf{q}}_{\chi}\hat{\gamma}_{2,1}\,\mathrm{d}\xi_1 = (\hat{\mathbf{q}}_{\chi}\hat{\gamma}_2)\Big|_{-1}^{1} - \int_{-1}^{1} \hat{\mathbf{q}}'_{\chi}\hat{\gamma}_2\,\mathrm{d}\xi_1 = -\int_{-1}^{1} \hat{\mathbf{q}}'_{\chi}\hat{\gamma}_2\,\mathrm{d}\xi_1. \tag{34}$$

4. Case III: magneto-elastic wave propagation in an infinite plate immersed in a transversal magnetic field

4.1. Governing system

The linear counterpart of the equations of motion of the geometrically nonlinear plate theory developed in Part 1 will be used to investigate the wave propagation of infinite plates in a transversal magnetic field. It is assumed that $\Theta_0 = 0$. As a result, the electrodynamic equations become

$$\bar{g}_{11}\varphi + \bar{g}_{12}\psi = \chi_{,2} - \frac{\gamma_2}{2h} - \Gamma_1, \tag{35a}$$

$$\bar{g}_{12}\varphi + \bar{g}_{22}\psi = -\chi_{,1} + \frac{\gamma_2}{2h} - \Gamma_2, \tag{35b}$$

$$\bar{g}_{11}\chi_{,11} + 2\bar{g}_{12}\chi_{,12} + \bar{g}_{22}\chi_{,22} - \mu\bar{\Xi}\dot{\chi} = \bar{g}_{12}\left[-\frac{1}{h}\gamma_{1,1} + \Gamma_{1,1} - \Gamma_{2,2}\right] + \bar{g}_{11}\left[\frac{1}{2h}\gamma_{2,1} - \Gamma_{2,1}\right] + \bar{g}_{22}\left[-\frac{1}{2h}\gamma_{1,2} + \Gamma_{1,2}\right]. \tag{35c}$$

In Eq. (35c), the relation defined by Eq. (35c) of Part 1 is used and γ_1, γ_2 are given as [4]

$$\gamma_1 = -\frac{1}{\pi}\int_{-\infty}^{\infty}\int_{-\infty}^{\infty}\frac{(x_2-s_2)\chi(s_1,s_2,t)\,\mathrm{d}s_1\,\mathrm{d}s_2}{[(x_1-s_1)^2+(x_2-s_2)^2]^{3/2}}, \tag{36a}$$

$$\gamma_2 = \frac{1}{\pi}\int_{-\infty}^{\infty}\int_{-\infty}^{\infty}\frac{(x_1-s_1)\chi(s_1,s_2,t)\,\mathrm{d}s_1\,\mathrm{d}s_2}{[(x_1-s_1)^2+(x_2-s_2)^2]^{3/2}}, \tag{36b}$$

while Γ_1, Γ_2 can be represented as

$$\Gamma_1 \equiv \bar{g}_{11}\dot{v}_2 B_{03}^0 - \bar{g}_{12}\dot{v}_1 B_{03}^0, \quad \Gamma_2 \equiv \bar{g}_{12}\dot{v}_2 B_{03}^0 - \bar{g}_{22}\dot{v}_1 B_{03}^0. \tag{37a, b}$$

From Eqs. (35) and (37), it is readily seen that χ, φ and ψ are functions of v_1, v_2 only.

The ponderomotive forces f_i $(i=1,2,3)$ are

$$f_1 = j_2 B_{03}^0, \quad f_2 = -j_1 B_{03}^0, \quad f_3 = 0, \tag{38a–c}$$

where, j_1 and j_2 reduce to:

$$j_1 = g_{11}^{(i)}[\varphi + \dot{v}_2 B_{03}^0] + g_{12}^{(i)}[\psi - \dot{v}_1 B_{03}^0] + x_3[g_{11}^{(i)}\dot{\beta}_2 - g_{12}^{(i)}\dot{\beta}_1]B_{03}^0, \quad x_3 \in [z_i, z_{i+1}), \tag{39a}$$

$$j_2 = g_{12}^{(i)}[\varphi + \dot{v}_2 B_{03}^0] + g_{22}^{(i)}[\psi - \dot{v}_1 B_{03}^0] + x_3[g_{12}^{(i)}\dot{\beta}_2 - g_{22}^{(i)}\dot{\beta}_1]B_{03}^0, \quad x_3 \in [z_i, z_{i+1}). \tag{39b}$$

As a result, the ponderomotive forces can be expressed as

$$\int_{-h}^{h} f_1\,\mathrm{d}x_3 = \sum_{k=1}^{N_L}\int_{z_i}^{z_{i+1}} f_1\,\mathrm{d}x_3 = 2h\left[-\chi_{,1} + \frac{\gamma_2}{2h} - \Gamma_2\right]B_{03}^0 + (B_{03}^0)^2 2h[\bar{g}_{12}\dot{v}_2 - \bar{g}_{22}\dot{v}_1], \tag{40a}$$

$$\int_{-h}^{h} f_2\,\mathrm{d}x_3 = \sum_{k=1}^{N_L}\int_{z_i}^{z_{i+1}} f_2\,\mathrm{d}x_3 = -2h\left[\chi_{,2} - \frac{\gamma_1}{2h} - \Gamma_2\right]B_{03}^0 - (B_{03}^0)^2 2h[\bar{g}_{11}\dot{v}_2 - \bar{g}_{12}\dot{v}_1], \tag{40b}$$

$$\int_{-h}^{h} x_3 f_1\,\mathrm{d}x_3 = [C_{12}^g\dot{\beta}_2 - C_{22}^g\dot{\beta}_1](B_{03}^0)^2, \quad \int_{-h}^{h} x_3 f_2\,\mathrm{d}x_3 = [-C_{11}^g\dot{\beta}_2 + C_{12}^g\dot{\beta}_1](B_{03}^0)^2. \tag{40c,d}$$

In Eqs. (40a–d), the parameters $C_{\alpha\beta}^g$ $(\alpha,\beta)=1,2$ are defined by Eq. (4a).

Associated to this case, the linear governing equations of the infinite plate become:

$$\begin{aligned}\delta v_1 : {} & (A_{11}v_{1,11} + 2A_{16}v_{1,12} + A_{66}v_{1,22}) + [A_{16}v_{2,11} + (A_{12}+A_{66})v_{2,12} + A_{26}v_{2,22}] \\ & - I_0\ddot{v}_1 + (2h\chi_{,1} - \gamma_2)B_{03}^0 = 0,\end{aligned} \tag{41a}$$

$$\begin{aligned}\delta v_2 : {} & [A_{16}v_{1,11} + (A_{12}+A_{66})v_{1,12} + A_{26}v_{1,22}] + (A_{66}v_{2,11} + 2A_{26}v_{2,12} + A_{22}v_{2,22}) \\ & - I_0\ddot{v}_2 - (2h\chi_{,2} - \gamma_1)B_{03}^0 = 0,\end{aligned} \tag{41b}$$

$$\begin{aligned}\delta v_3 : {} & A_{55}v_{3,11} + A_{45}v_{3,12} + A_{44}v_{3,22} + A_{55}\beta_{1,1} + A_{44}\beta_{2,2} + A_{45}(\beta_{2,1} + \beta_{1,2}) \\ & - I_0\ddot{v}_3 = 0,\end{aligned} \tag{41c}$$

$$\begin{aligned}\delta\beta_1 : {} & (D_{11}\beta_{1,11} + 2D_{16}\beta_{1,12} + D_{66}\beta_{1,22}) + [D_{16}\beta_{2,11} + (D_{12}+D_{66})\beta_{2,12} + D_{26}\beta_{2,22}] \\ & - A_{45}(\beta_2 + v_{3,2}) - A_{55}(\beta_1 + v_{3,1}) - I_2\ddot{\beta}_1 + (B_{03}^0)^2 C_{12}^g\dot{\beta}_2 - (B_{03}^0)^2 C_{22}^g\dot{\beta}_1 = 0,\end{aligned} \tag{41d}$$

$$\delta\beta_2 : [D_{16}\beta_{1,11} + (D_{16} + D_{66})\beta_{1,12} + D_{26}\beta_{1,22}] + (D_{22}\beta_{2,22} + 2D_{26}\beta_{2,12} + D_{66}\beta_{2,11}) - A_{44}(\beta_2 + v_{3,2}) - A_{45}(\beta_1 + v_{3,1}) - I_2\ddot{\beta}_2 - (B_{03}^0)^2 C_{11}^g \dot{\beta}_2 + (B_{03}^0)^2 C_{12}^g \dot{\beta}_1 = 0. \quad (41e)$$

Substituting Eqs. (37a,b) into Eq. (35c), the governing equation associated with χ can be simplified as

$$\bar{g}_{11}\chi_{,11} + 2\bar{g}_{12}\chi_{,12} + \bar{g}_{22}\chi_{,22} - \mu\bar{\Xi}\dot{\chi} = \left(-\frac{1}{h}\bar{g}_{12}\gamma_{1,1} + \frac{1}{2h}\bar{g}_{11}\gamma_{2,1} - \frac{1}{2h}\bar{g}_{22}\gamma_{1,2}\right) + \bar{\Xi}B_{03}^0(\dot{v}_{1,1} + \dot{v}_{2,2}). \quad (42)$$

Eqs. (41a–e), (42), together with Eqs. (36a,b) constitute the full set of governing equations of the infinite plate immersed in a transversal magnetic field. It is readily seen that this set of the governing equations splits into two uncoupled groups: one is associated with the flexural motion (v_3, β_α), and the other one associated with the in-plane motion (v_α).

4.2. Dispersion relation of the flexural waves

Consider the following solution form related to the flexural motion [1,6,7],

$$\begin{Bmatrix} v_3 \\ \beta_1 \\ \beta_2 \end{Bmatrix} = \begin{Bmatrix} v_3^0 \\ \beta_1^0 \\ \beta_2^0 \end{Bmatrix} \exp[\jmath\bar{k}(x_1\cos\wp + x_2\sin\wp) - \jmath\omega_\perp t], \quad (43)$$

and the following non-dimensional parameters:

$$\kappa \equiv \bar{k}h, \quad U_{\text{ref}} \equiv \sqrt{D_{11}/I_2}, \quad \hat{\omega}_\perp \equiv \frac{\omega_\perp h}{U_{\text{ref}}}, \quad \hat{v}_3^0 \equiv v_3^0/h. \quad (44a-d)$$

Then, the governing equations associated with the bending, as expressed in terms of v_3 and β_α, can be cast in the frequency domain in the following state-space form:

$$\hat{\omega}_\perp \begin{Bmatrix} \hat{v}_3^0 \\ \beta_1^0 \\ \beta_2^0 \\ \hat{\omega}_\perp\hat{v}_3^0 \\ \hat{\omega}_\perp\beta_1^0 \\ \hat{\omega}_\perp\beta_2^0 \end{Bmatrix} = \underbrace{\begin{bmatrix} 0 & 0 & 0 & 1 & 0 & 0 \\ 0 & 0 & 0 & 0 & 1 & 0 \\ 0 & 0 & 0 & 0 & 0 & 1 \\ \bar{\Lambda}_{41} & \bar{\Lambda}_{42} & \bar{\Lambda}_{43} & 0 & 0 & 0 \\ \bar{\Lambda}_{51} & \bar{\Lambda}_{52} & \bar{\Lambda}_{53} & 0 & \bar{\Lambda}_{55} & \bar{\Lambda}_{56} \\ \bar{\Lambda}_{61} & \bar{\Lambda}_{62} & \bar{\Lambda}_{63} & 0 & \bar{\Lambda}_{65} & \bar{\Lambda}_{66} \end{bmatrix}}_{\bar{\Lambda}} \begin{Bmatrix} \hat{v}_3^0 \\ \beta_1^0 \\ \beta_2^0 \\ \hat{\omega}_\perp\hat{v}_3^0 \\ \hat{\omega}_\perp\beta_1^0 \\ \hat{\omega}_\perp\beta_2^0 \end{Bmatrix}. \quad (45)$$

The coefficients in the form of $\bar{\Lambda}_{ij}$ in matrix $\bar{\Lambda}$ are defined in Appendix C. We note that the matrix $\bar{\Lambda}$ is function of κ and $\wp$.

Eq. (45) constitutes an eigenvalue problem (with the eigenvalue $\hat{\omega}_\perp$). Therefore, the dispersion relation of the flexural waves can be derived from the eigenvalue solution of Eq. (45).

4.3. Dispersion relation of the in-plane waves

Similar to the solution for the flexural waves as considered in the preceding section, we postulate the following solution form for the in-plane waves:

$$\begin{Bmatrix} v_1 \\ v_2 \\ \chi \end{Bmatrix} = \begin{Bmatrix} v_1^0 \\ v_2^0 \\ \chi^0 \end{Bmatrix} \exp[\jmath\bar{k}(x_1\cos\wp + x_2\sin\wp) - \jmath\omega_{\parallel}t]. \tag{46}$$

Based on Eq. (46) and the following non-dimensional parameters:

$$\hat{\omega}_{\parallel} \equiv \frac{\omega_{\parallel}h}{U_{\text{ref}}}, \quad \chi^0 \equiv \frac{\bar{\Xi}\sqrt{A_{11}I_0}hB_{03}^0}{\bar{g}_{11}}\hat{\chi}^0, \quad (\hat{v}_1^0;\hat{v}_2^0) \equiv (v_1^0, v_2^0)/h, \tag{47a–c}$$

where U_{ref} is defined by Eq. (44b), the governing equations associated with v_1, v_2 and χ can be cast in the following state-space form:

$$\hat{\omega}_{\parallel}\begin{Bmatrix} \hat{v}_1^0 \\ \hat{v}_2^0 \\ \hat{\chi}^0 \\ \hat{\omega}_{\parallel}\hat{v}_1^0 \\ \hat{\omega}_{\parallel}\hat{v}_2^0 \end{Bmatrix} = \underbrace{\begin{bmatrix} 0 & 0 & 0 & 1 & 0 \\ 0 & 0 & 0 & 0 & 1 \\ 0 & 0 & \tilde{\Lambda}_{33} & \tilde{\Lambda}_{34} & \tilde{\Lambda}_{35} \\ \tilde{\Lambda}_{41} & \tilde{\Lambda}_{42} & \tilde{\Lambda}_{43} & 0 & 0 \\ \tilde{\Lambda}_{51} & \tilde{\Lambda}_{52} & \tilde{\Lambda}_{53} & 0 & 0 \end{bmatrix}}_{\tilde{\Lambda}} \begin{Bmatrix} \hat{v}_1^0 \\ \hat{v}_2^0 \\ \hat{\chi}^0 \\ \hat{\omega}_{\parallel}\hat{v}_1^0 \\ \hat{\omega}_{\parallel}\hat{v}_2^0 \end{Bmatrix}. \tag{48}$$

The entries $\tilde{\Lambda}_{ij}$ in matrix $\tilde{\Lambda}$ are defined in Appendix C. As in the case of flexural waves, also here the matrix $\tilde{\Lambda}$ is function of κ and $\wp$. It is worth noting that when $\hat{\lambda} \ll 1$, the interactive influence of the induced outer magnetic field on the in-plane waves can be neglected.

5. Results and discussion

Fig. 2 displays the influence of the ply-angle on the dimensionless critical temperature, $\hat{\Theta}^{\star}$, and on the critical overdamped dimensionless temperature $\hat{\Theta}^{\text{od}}$, which are defined by Eqs. (23) and (24) and give the boundaries of thermal buckling and damped/over-damped vibrations, respectively. The involved elastic, thermal and electrical parameters are: $E_1/E_0 = 10$, $E_2/E_0 = 5$, $E_3/E_0 = 5$, $G_{12}/E_0 = 4$, $G_{23}/E_0 = 2$, $G_{13}/E_0 = 2$, $\mu_{12} = \mu_{23} = \mu_{13} = 0.25$, $\alpha_1/\alpha_0 = 0.1$, $\alpha_2/\alpha_0 = 2$, $\alpha_3/\alpha_0 = 1$, $E_0 = 10^{10}\,\text{N/m}^2$, $\alpha_0 = 10^{-3}$, $g_0 = 10^8\,\text{S/m}^3$. Unless otherwise stated, these prescribed parameters and the transversely shearable model (TS) will be used throughout Figs. 2–12. In Fig. 2, we notice the significant influence of lay-up and ply-angle on these two functions, implying that the tailoring technique can be used to efficiently control the vibrational behavior of the plate strip.

Fig. 3 shows the influence of the transversal magnetic field on $\hat{\Theta}^{\text{od}}$ for different lay-up configurations. It is remarked that among the four selected lay-up configurations, the one defined by $[90/45/0]_s$ yields the highest sensitivity of $\hat{\Theta}$ to the change of the magnetic field intensity, while $[0_6]$ yields the strongest resistance of $\hat{\Theta}$ to the variation of $\hat{B}_{03}^0$.

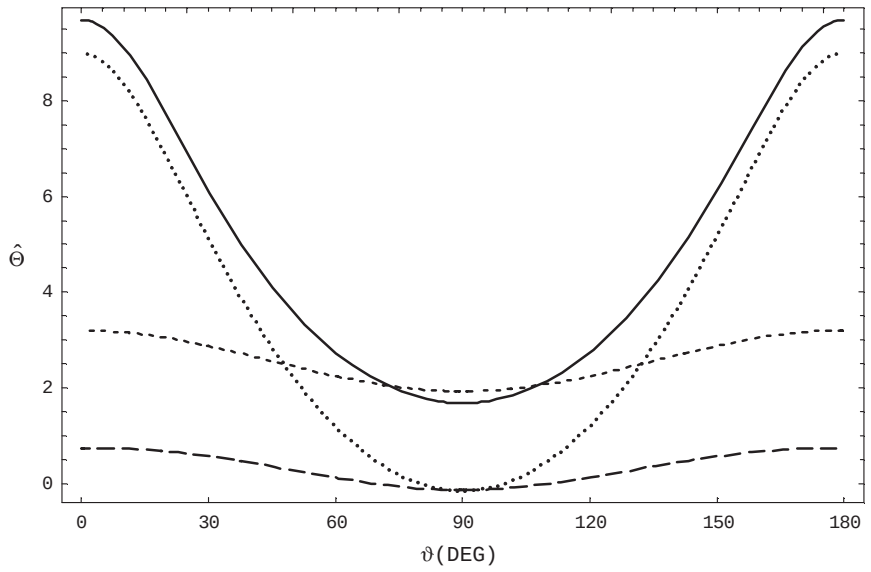

Fig. 2. Dependence of $\hat{\Theta}^{\star}$ and $\hat{\Theta}^{\mathrm{od}}$ on lamination and ply angle predicted by the NTS model. ($h/\ell_1 = 1/50, \hat{B}^0_{03} = 4.5, g_1/g_0 = 3.0, g_2/g_0 = 1.1, g_3/g_0 = 3.0$); ——, $\hat{\Theta}^{\star}$ in the case of $[0_6]$; ·····, $\hat{\Theta}^{\mathrm{od}}$ in the case of $[30_6]$; ------, $\hat{\Theta}^{\star}$ in the case of $[90_6]$; – – –, $\hat{\Theta}^{\mathrm{od}}$ in the case of $[90/45/0]_s$.

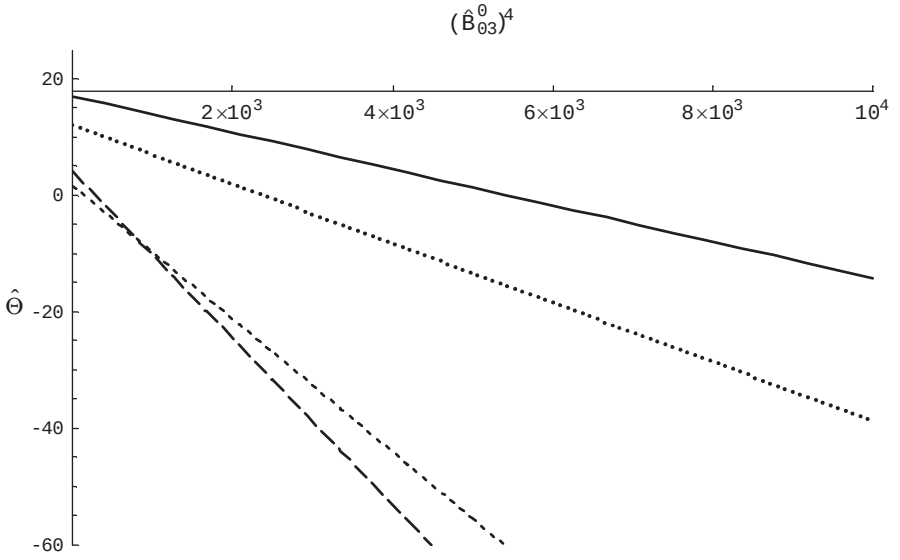

Fig. 3. Dependence of $\hat{\Theta}^{\mathrm{od}}$ on the magnetic field intensity parameter $\hat{B}^0_{03}$ predicted by the NTS model. ($h/\ell_1 = 1/50$, $g_1/g_0 = 3.0$, $g_2/g_0 = 1.1$, $g_3/g_0 = 3.0$); ——, $[0_6]$; ·····, $[30_6]$; ------, $[90_6]$; – – –, $[90/45/0]_s$.

Fig. 4 displays the influence of the magnetic field intensity parameter $\hat{B}^0_{03}$ on the vibration characteristics. It is recalled that $\mathrm{Re}[\lambda/\omega_0]$ corresponds to the damping coefficient, while $\mathrm{Im}[\lambda/\omega_0]$ corresponds to the oscillatory frequency. It is noted that the magnetic field intensity has a

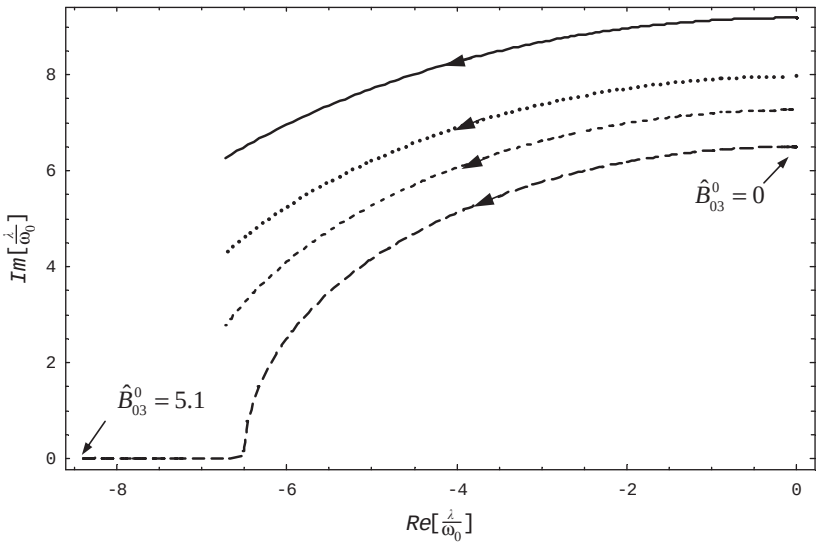

Fig. 4. Root loci of λ/ω_0 as $\hat{B}_{03}^0$ sweeps from 0 to 5.1 in the complex plane. (NTS model, $[90/45/0]_s$, $h/\ell_1 = 1/50$, $g_1/g_0 = 3.0$, $g_2/g_0 = 1.1$, $g_3/g_0 = 3.0$); ——, $\hat{\Theta} = -1.0$; ·····, $\hat{\Theta} = 0.0$; ------, $\hat{\Theta} = 0.5$; – – –, $\hat{\Theta} = 1.0$.

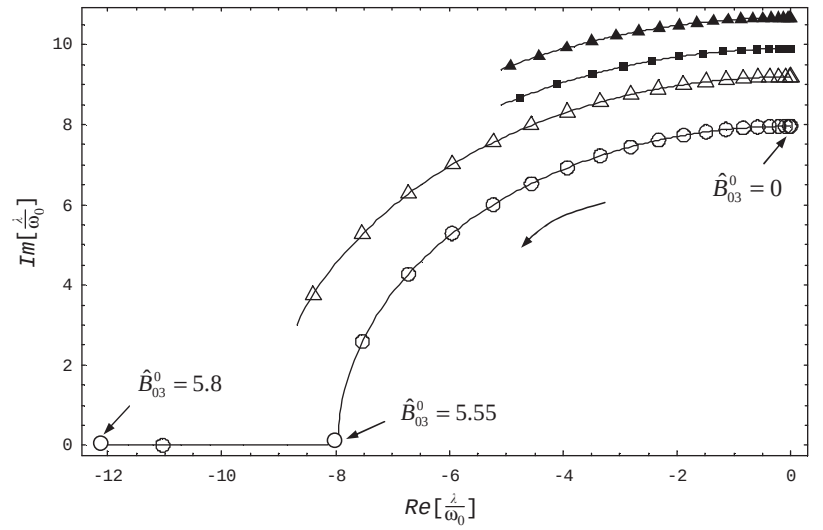

Fig. 5. Root loci of λ/ω_0 as $\hat{B}_{03}^0$ sweeps from 0 to 5.8 in the complex plane (NTS model, $h/\ell_1 = 1/50$, $g_1/g_0 = 3.0$, $g_2/g_0 = 1.1$, $g_3/g_0 = 3.0$); —○—, $\hat{\Theta} = 0$, $[90/45/0]_s$; - - -△- - -, $\hat{\Theta} = -1$, $[90/45/0]_s$; —■—, $\hat{\Theta} = 0$, $[30/-30/30]_s$; - - -▲- - -, $\hat{\Theta} = -1$, $[30/-30/30]_s$.

significant influence on both the damping coefficient and the frequency. Worthy of noting is also the fact that in the case $\hat{\Theta} = 1.0$, the plate strip experiences over-damped vibration, as indicated by the horizontal line segment.

Fig. 5 displays the influence of the magnetic field intensity parameter $\hat{B}_{03}^{0}$ on the vibration characteristics of the plate featuring different lay-up configurations. It is noted that among the selected lay-up configurations, the plate strip featuring $[90/45/0]_s$ displays the highest sensitivity to the variation of the intensity of the magnetic field. It is recalled in Fig. 3, the separator function $\hat{\Theta}^{\mathrm{od}}$ configured in the same lay-up experiences also the highest sensitivity to the change of the magnetic field.

Figs. 6–8 display the influence of transverse shear on plate-strip vibration with different thickness ratios. The convergence tests of the EGM in the solution of the first three eigenfrequencies of the plate strip by the TS and unshearable (NTS) models are listed in Tables 1 and 2, respectively. From Fig. 6, it can be concluded that for $h/\ell_1 = 1/50$, the transverse shear effect has a negligible influence on both the eigenfrequency and damping coefficient. However, with the increase of the thickness ratio h/ℓ_1, the influence of transverse shear effect on the eigenfrequency and damping becomes stronger. It is remarkable to note that in the case $h/\ell_1 = 1/12.5$, with the increase of $\hat{B}_{03}^{0}$ from 0 to 6.3, $\mathrm{Im}[\lambda_1/\omega_0]$ predicted by the unshearable model (NTS) drops from 5.56 to 3.94 (29% drop); however, $\mathrm{Im}[\lambda_1/\omega_0]$ predicted by the TS model drops only from 5.18 to 5.03 (2.9% drop). This implies that in such a case, the NTS model is no longer applicable and the transverse shear effect should be accounted for in the modeling.

Figs. 9–11 display the influence of the electroconductivity on the first three eigenvalues of free vibration of the plate strip. The significant influence of electroconductivity on the characteristics of the damped vibration becomes evident: in the case $g_0 = 10^8\,\mathrm{S/m^3}$ (see Fig. 9), the increase of $\hat{B}_{01}^{0}$ leads to the increase of $\mathrm{Im}[\lambda_i]$ $(i = \overline{1,3})$, while in the case $g_0 = 10^6\,\mathrm{S/m^3}$ (see Fig. 10), the increase of $\hat{B}_{01}^{0}$ leads to the decrease of $\mathrm{Im}[\lambda_1]$, but to the increase of $\mathrm{Im}[\lambda_2]$ and $\mathrm{Im}[\lambda_3]$; however, in

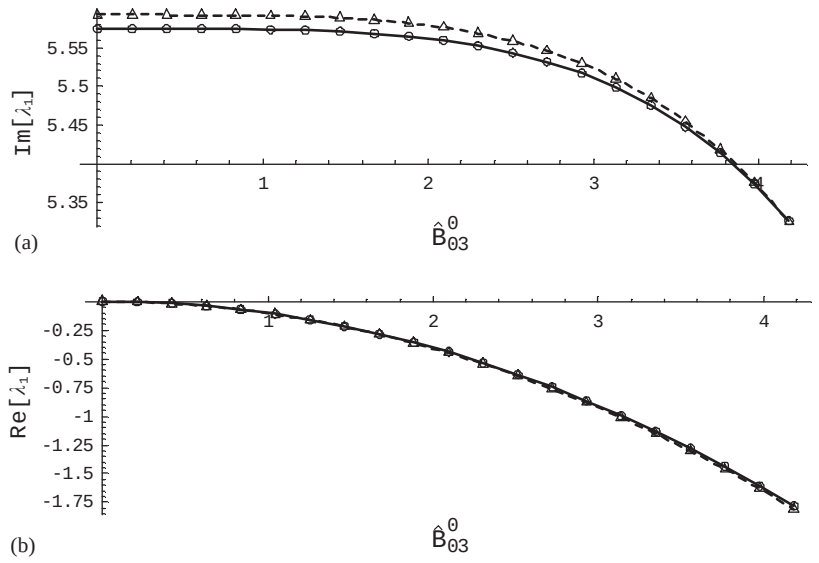

Fig. 6. Comparison of the TS and NTS models on the prediction of the fundamental eigenvalue λ_1 in Case I: (a) eigenvalue imaginary part $\mathrm{Im}[\lambda_1]$ versus $\hat{B}_{03}^{0}$; (b) eigenvalue real part $\mathrm{Re}[\lambda_1]$ versus $\hat{B}_{03}^{0}$. ($[0_6]$, $h/\ell_1 = 1/50$, $g_1/g_0 = 3.0$, $g_2/g_0 = 1.1$, $g_3/g_0 = 3.0$); $N_m = 10$ for the NTS model (---△---) and $N_m = 20$ for the TS model (—○—).

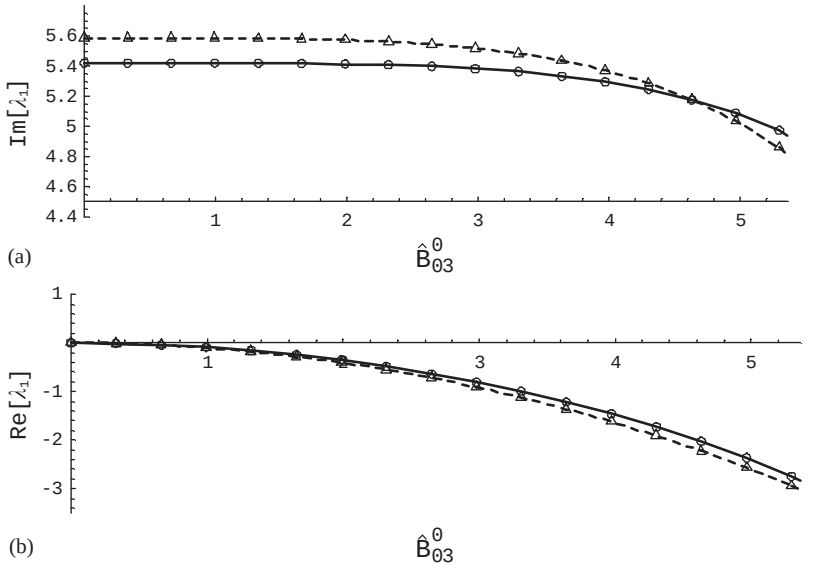

Fig. 7. Comparison of the TS and NTS models on the prediction of the fundamental eigenvalue λ_1 in Case I: (a) eigenvalue imaginary part Im[λ_1] versus $\hat{B}^0_{03}$; (b) eigenvalue real part Re[λ_1] versus $\hat{B}^0_{03}$. ([0_6], $h/\ell_1 = 1/20$, $g_1/g_0 = 3.0$, $g_2/g_0 = 1.1$, $g_3/g_0 = 3.0$); $N_m = 10$ for the NTS model (---△---) and $N_m = 20$ for the TS model (—○—).

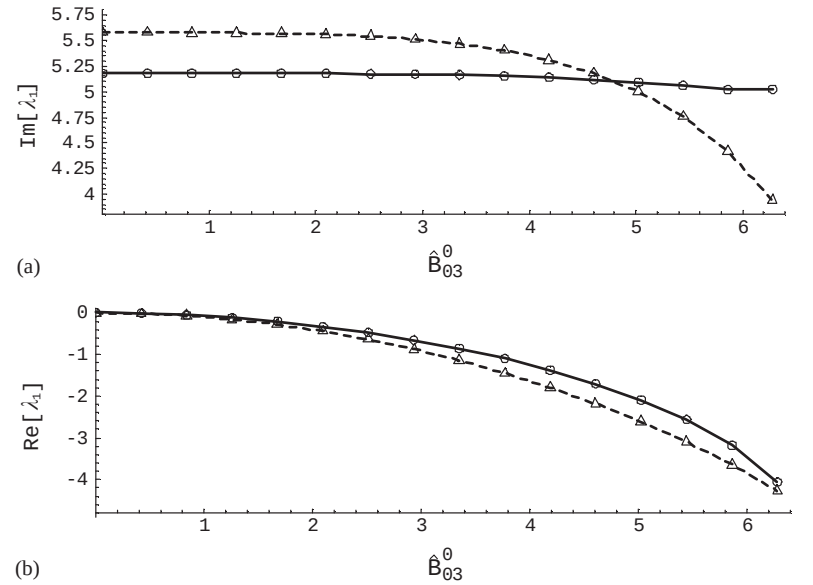

Fig. 8. Comparison of the TS and NTS models on the prediction of the fundamental eigenvalue λ_1 in Case I: (a) eigenvalue imaginary part Im[λ_1] versus $\hat{B}^0_{03}$; (b) eigenvalue real part Re[λ_1] versus $\hat{B}^0_{03}$. ([0_6], $h/\ell_1 = 1/12.5$, $g_1/g_0 = 3.0$, $g_2/g_0 = 1.1$, $g_3/g_0 = 3.0$); $N_m = 10$ for the NTS model (---△---) and $N_m = 20$ for the TS model (—○—).

Table 1
Convergence of the EGM in the solution of the first three eigenfrequencies of the plate strip used in Figs. 6–8 by the TS model ($[0_6], \hat{B}_{03}^0 = 0$)

N_m	$\hat{\omega}_1$	$\hat{\omega}_2$	$\hat{\omega}_3$
4	6.025	32.424	80.333
6	5.606	29.124	68.017
8	5.557	28.850	67.302
10	5.536	28.739	67.032
12	5.526	28.686	66.907
14	5.520	28.658	66.842
16	5.517	28.641	66.804
18	5.515	28.631	66.781
20	5.514	28.624	66.766

Table 2
Convergence of the EGM in the solution of the first three eigenfrequencies of the plate strip used in Figs. 6–8 by the NTS model ($[0_6], \hat{B}_{03}^0 = 0$)

N_m	$\hat{\omega}_1$	$\hat{\omega}_2$	$\hat{\omega}_3$
4	5.597	30.310	75.139
5	5.595	30.250	74.761
6	5.594	30.221	74.583
7	5.593	30.205	74.489
8	5.593	30.196	74.434
9	5.593	30.191	74.400
10	5.593	30.187	74.377

the case $g_0 = 10^5\,\mathrm{S/m^3}$, the increase of $\hat{B}_{01}^0$ yields the decrease of $\mathrm{Im}[\lambda_i]$ $(i = \overline{1,3})$. This phenomenon can be explained by the fact that the magnetic field modifies not only the structural damping, but also its stiffness. The strong influence of the magnetic field on the vibration is also manifested by the vibrational damping coefficient, as displayed in Fig. 12. Depending on the magnetic field intensity parameter $\hat{B}_{01}$, the order of the eigenmodes in terms of the amplitude of their damping coefficients varies.

Figs. 13 and 14 display the dispersion relation of the flexural magneto-elastic waves within an infinite plate. The related parameters are: $[90/45/0]_s$, $E_1/E_0 = 10$, $E_2/E_0 = 2$, $E_3/E_0 = 2$, $G_{12}/E_0 = 2$, $G_{23}/E_0 = 4$, $G_{13}/E_0 = 4$, $\mu_{12} = \mu_{23} = \mu_{13} = 0.25$, $\alpha_1/\alpha_0 = 0.1$, $\alpha_2/\alpha_0 = 2$, $\alpha_3/\alpha_0 = 1$, $g_1/g_0 = 3$, $g_2/g_0 = 1.1$, $g_3/g_0 = 1$, $E_0 = 10^{10}\,\mathrm{N/m^2}$, $\alpha_0 = 10^{-3}$, $g_0 = 10^8\,\mathrm{S/m^3}$ (these parameters will also be applied in Fig. 15). From Fig. 13, it can be seen that for $\kappa > 1.5$, there is almost no dispersion for the flexural magneto-elastic waves, while Fig. 14 shows that $(\hat{\omega}_\perp)_2$ features the highest damping.

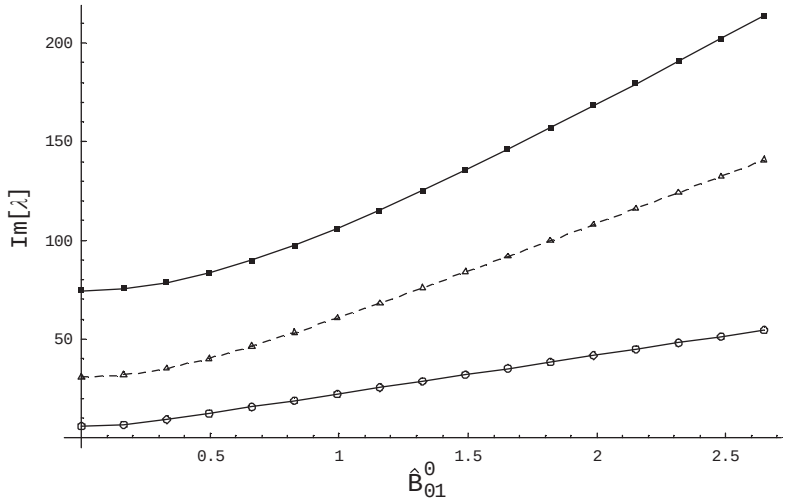

Fig. 9. The variation of $\mathrm{Im}[\lambda_1]$ (—○—), $\mathrm{Im}[\lambda_2]$ (---△---) and $\mathrm{Im}[\lambda_3]$ (—■—) of a plate strip as a function of $\hat{B}_{01}^{0}$. ($[90/45/0]_s$, $h/\ell_1 = 1/50$, $g_1/g_0 = 3.0$, $g_2/g_0 = 1.1$, $g_3/g_0 = 1.0$, $g_0 = 10^8\,\mathrm{S/m^3}$.)

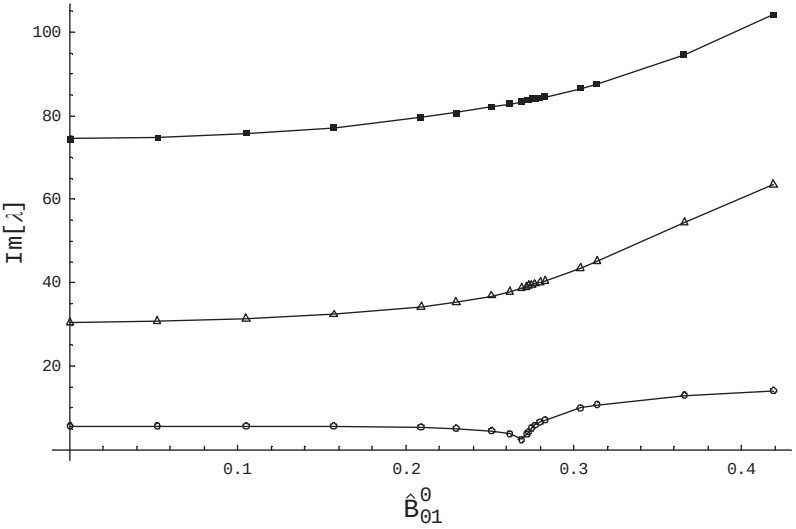

Fig. 10. The variation of $\mathrm{Im}[\lambda_1]$ (—○—), $\mathrm{Im}[\lambda_2]$ (—△—) and $\mathrm{Im}[\lambda_3]$ (—■—) of a plate strip as a function of $\hat{B}_{01}^{0}$. ($[90/45/0]_s$, $h/\ell_1 = 1/50$, $g_1/g_0 = 3.0$, $g_2/g_0 = 1.1$, $g_3/g_0 = 3.0$, $g_0 = 10^6\,\mathrm{S/m^3}$.)

Fig. 15 displays the influence of the magnetic field on the dispersion curve $\mathrm{Re}[\hat{\omega}_\perp]$ versus κ. It can be seen that among the three waves, the frequency corresponding to $(\hat{\omega}_\perp)_2$ is the most sensitive to the variation of the magnetic field.

Since the magnetic field has negligible influence on the in-plane magneto-elastic waves within an infinite plate, the numerical results will be omitted here.

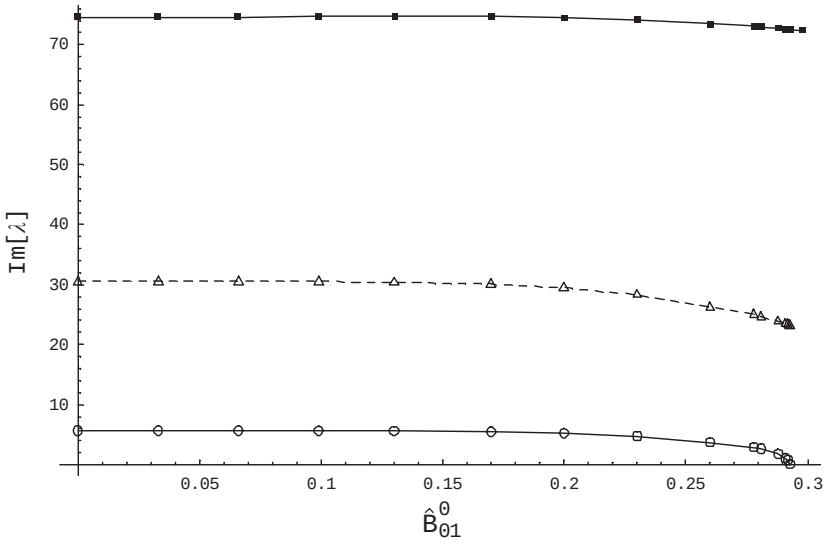

Fig. 11. The variation of Im[λ_1] (—○—), Im[λ_2] (---△---) and Im[λ_3] (—■—) of a plate strip as a function of $\hat{B}_{01}^{0}$. ($[90/45/0]_s$, $h/\ell_1 = 1/50$, $g_1/g_0 = 3.0$, $g_2/g_0 = 1.1$, $g_3/g_0 = 3.0$, $g_0 = 10^5\,\mathrm{S/m^3}$.)

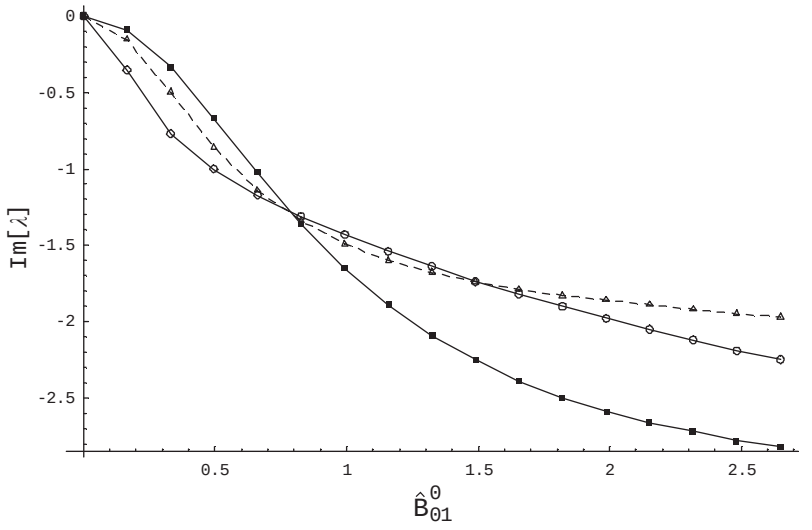

Fig. 12. Damping coefficients corresponding to the first three eigenmodes of a plate strip versus $\hat{B}_{01}^{0}$. ($[90/45/0]_s$, $h/\ell_1 = 1/50$, $g_1/g_0 = 5.0$, $g_2/g_0 = 3.0$, $g_3/g_0 = 1.0$, $g_0 = 10^8\,\mathrm{S/m^3}$); —○—, Re[$\lambda_1$]; ---△---, Re[$\lambda_2$]; —■—, Re[$\lambda_3$].

6. Concluding remarks

- In the special magneto-elastic cases investigated here, an exact split of the full set of governing equations into two groups is featured: one group is associated with stretching and involves v_1,

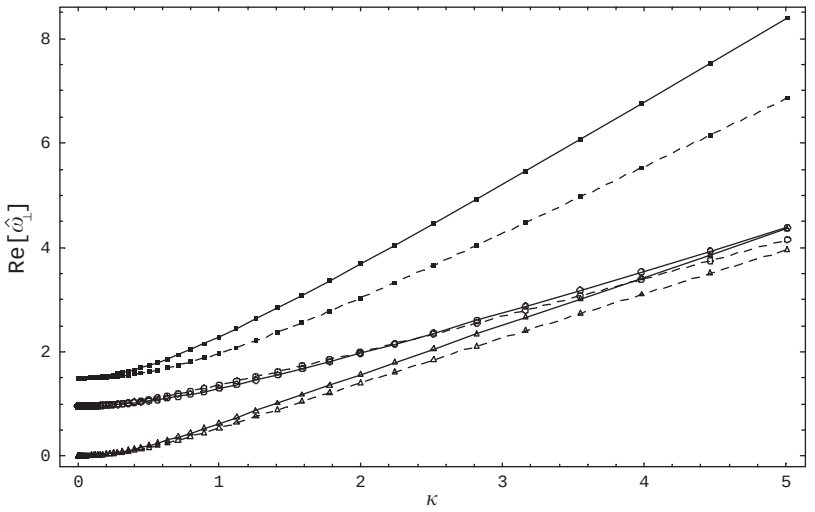

Fig. 13. Dispersion relation of the flexural magnetoelastic waves within an infinite plate: Re[$\hat{\omega}_\perp$] versus κ. ($\hat{B}_{03}^0 = 2.1$); —△—, Re[$(\hat{\omega}_\perp)_1$], $\wp = 70°$; —○—, Re[$(\hat{\omega}_\perp)_2$], $\wp = 70°$; —■—, Re[$(\hat{\omega}_\perp)_3$], $\wp = 70°$; - - -△- - -, Re[$(\hat{\omega}_\perp)_1$], $\wp = 30°$; - - -○- - -, Re[$(\hat{\omega}_\perp)_2$], $\wp = 30°$; - - -■- - -, Re[$(\hat{\omega}_\perp)_3$], $\wp = 30°$.

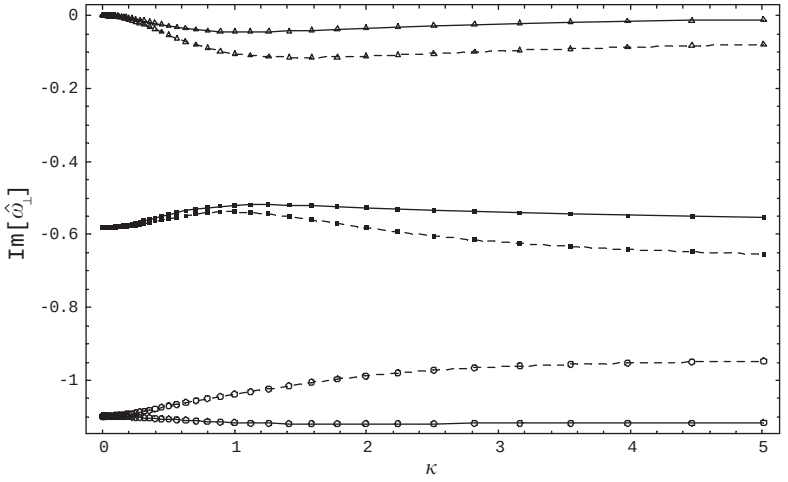

Fig. 14. Dispersion relation of the flexural magnetoelastic waves within an infinite plate: Im[$\hat{\omega}_\perp$] versus κ. ($\hat{B}_{03}^0 = 2.1$); —△—, Re[$(\hat{\omega}_\perp)_1$], $\wp = 70°$; —○—, Re[$(\hat{\omega}_\perp)_2$], $\wp = 70°$; —■—, Re[$(\hat{\omega}_\perp)_3$], $\wp = 70°$; - - -△- - -, Re[$(\hat{\omega}_\perp)_1$], $\wp = 30°$; - - -○- - -, Re[$(\hat{\omega}_\perp)_2$], $\wp = 30°$; - - -■- - -, Re[$(\hat{\omega}_\perp)_3$], $\wp = 30°$.

v_2, χ, and the induced outside magnetic field represented in terms of γ_1, γ_2; and the other group that is associated with the bending expressed in terms of v_3, β_1 and β_2.

- For moderately thick plates (e.g., $h/\ell \geqslant 1/12.5$), the transverse shear effects must be included in order to get reliable results.

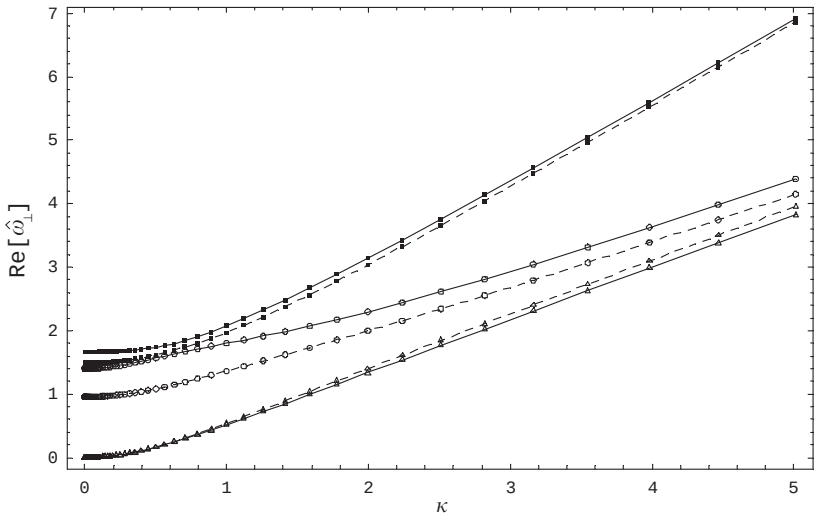

Fig. 15. Dispersion relation of the flexural magnetoelastic waves within an infinite plate: Re[$\hat{\omega}_\perp$] versus κ. ($\wp = 30^\circ$); —△—, Re[$(\hat{\omega}_\perp)_1$], $\hat{B}^0_{03} = 0$; —○—, Re[$(\hat{\omega}_\perp)_2$], $\hat{B}^0_{03} = 2.1$; —■—, Re[$(\hat{\omega}_\perp)_3$], $\hat{B}^0_{03} = 0$; - - -△- - -, Re[$(\hat{\omega}_\perp)_1$], $\hat{B}^0_{03} = 2.1$; - - -○- - -, Re[$(\hat{\omega}_\perp)_2$], $\hat{B}^0_{03} = 0$; - - -■- - -, Re[$(\hat{\omega}_\perp)_3$], $\hat{B}^0_{03} = 2.1$.

- The influence of the transversal magnetic field on vibration is manifested only by the damping effect; however, the axial magnetic field modifies not only the damping, but also the stiffness.
- Finite electroconductivity has a significant and complex influence on the vibrational behavior of plate strips. Contrary to the case of perfectly electroconductive plates, in the case of finite electroconductivity, the magnetic field may decrease the eigenfrequencies. Furthermore, the magnetic field may reorder the sequence of the eigenmodes in terms of the amplitude of the their damping coefficients. This phenomenon can have significant implications on the active control of such type of structures.

Acknowledgements

The partial support of NASA Langley Research Center through Grant NAG-01101 is gratefully acknowledged.

Appendix A. Definition of matrices in Eqs. (15) and (18)

$$\mathbf{M}_{qq} \equiv \frac{I_2 h^2}{I_0 \ell_1^2} \int_{-1}^{1} \hat{\mathbf{\Psi}}' \hat{\mathbf{\Psi}}'^{\mathrm{T}} \, \mathrm{d}\xi_1 + \int_{-1}^{1} \hat{\mathbf{\Psi}} \hat{\mathbf{\Psi}}^{\mathrm{T}} \, \mathrm{d}\xi_1, \quad \mathbf{C}_{qq} \equiv \frac{(B^0_{03})^2 C^g_{22}}{\sqrt{D_{11} I_0}} \int_{-1}^{1} \hat{\mathbf{\Psi}} \hat{\mathbf{\Psi}}'^{\mathrm{T}} \, \mathrm{d}\xi_1,$$

$$\mathbf{K}_{qq} \equiv \int_{-1}^{1} \hat{\mathbf{\Psi}}'' \hat{\mathbf{\Psi}}''^{\mathrm{T}} \, \mathrm{d}\xi_1 - \Theta \frac{A^\alpha_{11} \ell_1^2}{D_{11}} \int_{-1}^{1} \hat{\mathbf{\Psi}}' \hat{\mathbf{\Psi}}'^{\mathrm{T}} \, \mathrm{d}\xi_1,$$

$$\mathbf{M}_{vv} \equiv \frac{I_0 h^2}{I_2}\int_{-1}^{1} \hat{\mathbf{\Psi}}_v \hat{\mathbf{\Psi}}_v^{\mathrm{T}}\,\mathrm{d}\xi_1, \quad \mathbf{M}_{\beta_1\beta_1} \equiv \int_{-1}^{1} \hat{\mathbf{\Psi}}_{\beta_1} \hat{\mathbf{\Psi}}_{\beta_1}^{\mathrm{T}}\,\mathrm{d}\xi_1, \quad \mathbf{M}_{\beta_2\beta_2} \equiv \int_{-1}^{1} \hat{\mathbf{\Psi}}_{\beta_2} \hat{\mathbf{\Psi}}_{\beta_2}^{\mathrm{T}}\,\mathrm{d}\xi_1,$$

$$\mathbf{K}_{vv} \equiv \frac{A_{55}\ell_1^2 I_0 h^2}{D_{11} I_2}\int_{-1}^{1} \hat{\mathbf{\Psi}}_v' \hat{\mathbf{\Psi}}_v'^{\mathrm{T}}\,\mathrm{d}\xi_1, \quad \mathbf{K}_{v\beta_1} \equiv \frac{A_{55}\ell_1^4 I_0}{D_{11} I_2}\left(\frac{h}{\ell_1}\right)\int_{-1}^{1} \hat{\mathbf{\Psi}}_v' \hat{\mathbf{\Psi}}_{\beta_1}^{\mathrm{T}}\,\mathrm{d}\xi_1,$$

$$\mathbf{K}_{v\beta_2} \equiv \frac{A_{45}\ell_1^4 I_0}{D_{11} I_2}\left(\frac{h}{\ell_1}\right)\int_{-1}^{1} \hat{\mathbf{\Psi}}_v' \hat{\mathbf{\Psi}}_{\beta_2}^{\mathrm{T}}\,\mathrm{d}\xi_1, \quad \mathbf{K}_{\beta_1\beta_1} \equiv \frac{I_0 \ell_1^2}{I_2}\int_{-1}^{1} \hat{\mathbf{\Psi}}_{\beta_1}' \hat{\mathbf{\Psi}}_{\beta_1}'^{\mathrm{T}}\,\mathrm{d}\xi_1 + \frac{A_{55}\ell_1^4 I_0}{I_2 D_{11}}\int_{-1}^{1} \hat{\mathbf{\Psi}}_{\beta_1} \hat{\mathbf{\Psi}}_{\beta_1}^{\mathrm{T}}\,\mathrm{d}\xi_1,$$

$$\mathbf{K}_{\beta_1\beta_2} \equiv \frac{D_{16} I_0 \ell_1^2}{D_{11} I_2}\int_{-1}^{1} \hat{\mathbf{\Psi}}_{\beta_1}' \hat{\mathbf{\Psi}}_{\beta_2}'^{\mathrm{T}}\,\mathrm{d}\xi_1 + \frac{A_{45}\ell_1^4 I_0}{I_2 D_{11}}\int_{-1}^{1} \hat{\mathbf{q}}_{\beta_1} \hat{\mathbf{\Psi}}_{\beta_2}^{\mathrm{T}}\,\mathrm{d}\xi_1,$$

$$\mathbf{K}_{\beta_2\beta_2} \equiv \frac{D_{66} I_0 \ell_1^2}{D_{11} I_2}\int_{-1}^{1} \hat{\mathbf{\Psi}}_{\beta_2}' \hat{\mathbf{\Psi}}'^{\mathrm{T}}_{\beta_2}\,\mathrm{d}\xi_1 + \frac{A_{44}\ell_1^4 I_0}{I_2 D_{11}}\int_{-1}^{1} \hat{\mathbf{\Psi}}_{\beta_2} \hat{\mathbf{\Psi}}_{\beta_2}^{\mathrm{T}}\,\mathrm{d}\xi_1,$$

$$\mathbf{C}_{\beta_1\beta_1} \equiv (B_{03}^0)^2\,\frac{C_{22}^g \ell_1^2 \sqrt{I_0}}{I_2\sqrt{D_{11}}}\int_{-1}^{1} \hat{\mathbf{\Psi}}_{\beta_1} \hat{\mathbf{\Psi}}_{\beta_1}^{\mathrm{T}}\,\mathrm{d}\xi_1, \quad \mathbf{C}_{\beta_1\beta_2} \equiv -(B_{03}^0)^2\,\frac{C_{12}^g \ell_1^2 \sqrt{I_0}}{I_2\sqrt{D_{11}}}\int_{-1}^{1} \hat{\mathbf{\Psi}}_{\beta_1} \hat{\mathbf{\Psi}}_{\beta_2}^{\mathrm{T}}\,\mathrm{d}\xi_1,$$

$$\mathbf{C}_{\beta_2\beta_2} \equiv (B_{03}^0)^2\,\frac{C_{11}^g \ell_1^2 \sqrt{I_0}}{I_2\sqrt{D_{11}}}\int_{-1}^{1} \hat{\mathbf{\Psi}}_{\beta_2} \hat{\mathbf{\Psi}}_{\beta_2}^{\mathrm{T}}\,\mathrm{d}\xi_1, \quad \mathbf{C}_{\beta_2\beta_1} = \mathbf{C}_{\beta_1\beta_2}^{\mathrm{T}},$$

$$\mathbf{K}_{\beta_1 v} = \mathbf{K}_{v\beta_1}^{\mathrm{T}}, \quad \mathbf{K}_{\beta_2 v} = \mathbf{K}_{v\beta_2}^{\mathrm{T}}, \quad \mathbf{K}_{\beta_2\beta_1} = \mathbf{K}_{\beta_1\beta_2}^{\mathrm{T}}.$$

Appendix B. Definition of matrices in Eq. (33)

$$\mathbf{K}_{v\chi} \equiv -\frac{(B_{01}^0)^2 2h^3 \bar{g}_{11}}{I_2\omega_0}\left[\frac{\bar{\Xi}}{\bar{g}_{11}^2}\frac{1}{\pi}\int_{-1}^{1}\frac{\hat{\mathbf{\Psi}}_v(\xi_1)\,\mathrm{d}\xi_1}{\sqrt{1-\xi_1^2}}\int_{-1}^{1}\frac{\sqrt{1-\xi_s^2}}{\xi_s-\xi_1}\,\hat{\mathbf{\Psi}}_\chi(\xi_s)\,\mathrm{d}\xi_s + 2\,\frac{I_0 h^2}{I_2}\left(\frac{h}{\ell_1}\right)\int_{-1}^{1}\hat{\mathbf{\Psi}}_v \hat{\mathbf{\Psi}}_\chi'^{\mathrm{T}}\,\mathrm{d}\xi_1\right],$$

$$\mathbf{K}_{\beta_2\chi} \equiv \frac{(B_{01}^0)^2 2h^3 \bar{g}_{11}}{I_2\omega_0}\left[\frac{C_{11}^g}{4h^3\bar{g}_{11}}\frac{\bar{g}_{12}}{\bar{g}_{11}} - \frac{C_{12}^g}{4h^3\bar{g}_{11}}\right]\int_{-1}^{1}\hat{\mathbf{\Psi}}_{\beta_2}\hat{\mathbf{\Psi}}_\chi^{\mathrm{T}}\,\mathrm{d}\xi_1\left[\int_{-1}^{1}\hat{\mathbf{\Psi}}_\chi\hat{\mathbf{\Psi}}_\chi^{\mathrm{T}}\,\mathrm{d}\xi_1\right]^{-1}\mathbf{B}_\chi,$$

$$\mathbf{C}_{\beta_2 v} \equiv \frac{(B_{01}^0)^2 2h^3 \bar{g}_{11}}{I_2\omega_0}\left[\frac{C_{11}^g}{4h^3\bar{g}_{11}}\frac{\bar{g}_{12}}{\bar{g}_{11}} - \frac{C_{12}^g}{4h^3\bar{g}_{11}}\right]\left[\left(\frac{h}{\ell_1}\right)\int_{-1}^{1}\hat{\mathbf{\Psi}}_{\beta_2}\hat{\mathbf{\Psi}}_v'^{\mathrm{T}}\,\mathrm{d}\xi_1 - \left(\int_{-1}^{1}\hat{\mathbf{\Psi}}_{\beta_2}\hat{\mathbf{\Psi}}_\chi^{\mathrm{T}}\,\mathrm{d}\xi_1\right)\left(\int_{-1}^{1}\hat{\mathbf{\Psi}}_\chi\hat{\mathbf{\Psi}}_\chi^{\mathrm{T}}\,\mathrm{d}\xi_1\right)^{-1}\mathbf{C}_\chi\right],$$

$$\mathbf{A}_\chi \equiv \frac{\mu_0 \bar{\Xi} \omega_0 h^2}{\bar{g}_{11}} \int_{-1}^{1} \hat{\mathbf{\Psi}}_\chi \hat{\mathbf{\Psi}}_\chi^{\mathrm{T}} \, \mathrm{d}\xi_1, \quad \mathbf{C}_\chi \equiv \left(\frac{h}{\ell_1}\right) \int_{-1}^{1} \hat{\mathbf{\Psi}}_\chi \hat{\mathbf{\Psi}}_v'^{\mathrm{T}} \, \mathrm{d}\xi_1,$$

$$\mathbf{B}_\chi \equiv \left(\frac{h}{\ell_1}\right)^2 \int_{-1}^{1} \hat{\mathbf{\Psi}}_\chi' \hat{\mathbf{\Psi}}_\chi'^{\mathrm{T}} \, \mathrm{d}\xi_1 + \left(\frac{h}{\ell_1}\right) \frac{1}{\pi} \int_{-1}^{1} \frac{\hat{\mathbf{\Psi}}_\chi'(\xi_1) \, \mathrm{d}\xi_1}{\sqrt{1-\xi_1^2}} \int_{-1}^{1} \frac{\sqrt{1-\xi_s^2}}{\xi_s - \xi_1} \hat{\mathbf{\Psi}}_\chi^{\mathrm{T}}(\xi_s) \, \mathrm{d}\xi_s.$$

Appendix C. Expression of the coefficients in Eqs. (45) and (48)

$$\bar{\Lambda}_{41} \equiv \frac{I_2}{I_0 h^2} \left(\frac{A_{55} h^2}{D_{11}} \cos^2 \wp + \frac{2A_{45} h^2}{2D_{11}} \sin 2\wp + \frac{A_{44} h^2}{D_{11}} \sin^2 \wp \right) \kappa^2,$$

$$\bar{\Lambda}_{42} \equiv -\jmath \left(\frac{A_{55} I_2}{D_{11} I_0} \cos \wp + \frac{A_{45} I_2}{D_{11} I_0} \sin \wp \right) \kappa, \quad \bar{\Lambda}_{43} \equiv -\jmath \left(\frac{A_{44} I_2}{D_{11} I_0} \sin \wp + \frac{A_{45} I_2}{D_{11} I_0} \cos \wp \right) \kappa,$$

$$\bar{\Lambda}_{51} \equiv \jmath \left(\frac{A_{45} h^2}{D_{11}} \sin \wp + \frac{A_{55} h^2}{D_{11}} \cos \wp \right) \kappa,$$

$$\bar{\Lambda}_{52} \equiv \left(\cos^2 \wp + \frac{D_{16}}{D_{11}} \sin 2\wp + \frac{D_{66}}{D_{11}} \sin^2 \wp \right) \kappa^2 + \frac{A_{55} h^2}{D_{11}},$$

$$\bar{\Lambda}_{55} \equiv -\jmath \frac{C_{22}^g (B_{03}^0)^2 h}{\sqrt{D_{11} I_2}}, \quad \bar{\Lambda}_{56} \equiv \jmath \frac{C_{12}^g (B_{03}^0)^2 h}{\sqrt{D_{11} I_2}},$$

$$\bar{\Lambda}_{53} \equiv \left[\frac{D_{16}}{D_{11}} \cos^2 \wp + \frac{(D_{12} + D_{66})}{2D_{11}} \sin 2\wp + \frac{D_{26}}{D_{11}} \sin^2 \wp \right] \kappa^2 + \frac{A_{45} h^2}{D_{11}},$$

$$\bar{\Lambda}_{61} \equiv \jmath \left(\frac{A_{44} h^2}{D_{11}} \sin \wp + \frac{A_{45} h^2}{D_{11}} \cos \wp \right) \kappa,$$

$$\bar{\Lambda}_{62} \equiv \left[\frac{D_{16}}{D_{11}} \cos^2 \wp + \frac{(D_{16} + D_{66})}{2D_{11}} \sin 2\wp + \frac{D_{26}}{D_{11}} \sin^2 \wp \right] \kappa^2 + \frac{A_{45} h^2}{D_{11}},$$

$$\bar{\Lambda}_{65} \equiv \jmath \frac{C_{12}^g (B_{03}^0)^2 h}{\sqrt{D_{11} I_2}}, \quad \bar{\Lambda}_{66} \equiv -\jmath \frac{C_{11}^g (B_{03}^0)^2 h}{\sqrt{D_{11} I_2}},$$

$$\bar{\Lambda}_{63} \equiv \left(\frac{D_{22}}{D_{11}} \sin^2 \wp + \frac{2D_{26}}{D_{11}} \sin 2\wp + \frac{D_{66}}{D_{11}} \cos^2 \wp \right) \kappa^2 + \frac{A_{44} h^2}{D_{11}},$$

$$\tilde{\Lambda}_{34} \equiv -\jmath \frac{\bar{g}_{11}}{\mu_0 \bar{\Xi} h \sqrt{A_{11}/I_0}} \kappa \cos \wp, \quad \tilde{\Lambda}_{35} \equiv -\jmath \frac{\bar{g}_{11}}{\mu_0 \bar{\Xi} h \sqrt{A_{11}/I_0}} \kappa \sin \wp,$$

$$\tilde{\Lambda}_{33} \equiv -\jmath \frac{\bar{g}_{11}}{\mu_0 \bar{\Xi} h \sqrt{A_{11}/I_0}} (\kappa^2 + \kappa)\left(\cos^2 \wp + \frac{\bar{g}_{12}}{\bar{g}_{11}} \sin 2\wp + \frac{\bar{g}_{22}}{\bar{g}_{11}} \sin^2 \wp\right),$$

$$\tilde{\Lambda}_{41} \equiv \left(\cos^2 \wp + \frac{A_{16}}{A_{11}} \sin 2\wp + \frac{A_{66}}{A_{11}} \sin^2 \wp\right)\kappa^2,$$

$$\tilde{\Lambda}_{42} \equiv \left(\frac{A_{16}}{A_{11}} \cos^2 \wp + \frac{A_{12} + A_{66}}{2A_{11}} \sin 2\wp + \frac{A_{26}}{A_{11}} \sin^2 \wp\right)\kappa^2,$$

$$\tilde{\Lambda}_{43} \equiv 2\jmath(\kappa + 1) \cos \wp \frac{(B^0_{03})^2 h^2 \bar{\Xi}}{\sqrt{A_{11} I_0} \bar{g}_{11}}, \quad \tilde{\Lambda}_{51} \equiv \tilde{\Lambda}_{42}$$

$$\tilde{\Lambda}_{52} \equiv \left(\frac{A_{66}}{A_{11}} \cos^2 \wp + \frac{A_{26}}{A_{11}} \sin 2\wp + \frac{A_{22}}{A_{11}} \sin^2 \wp\right)\kappa^2,$$

$$\tilde{\Lambda}_{53} \equiv 2\jmath(\kappa - 1) \sin \wp \frac{(B^0_{03})^2 h^2 \bar{\Xi}}{\sqrt{A_{11} I_0} \bar{g}_{11}}.$$

References

[1] J.D. Achenbach, *Wave Propagation in Elastic Solids*, North-Holland, New York, 1973, pp. 122–127.

[2] R.L. Bisplinghoff, H. Ashley, R.L. Halfman, *Aeroelasticity*, Dover Publications, New York, 1996, pp. 206–208, 221–225.

[3] F.D. Gakhov, *Boundary Value Problems* (I.N. Sneddon, Trans.), Addison-Wesley, Reading, MA, 1966, pp. 426–428.

[4] L. Librescu, D. Hasanyan, Z. Qin, D. Ambur, Nonlinear magneto-thermo-elasticity of anisotropic plates immersed in a magnetic field, *Journal of Thermal Stresses* 26 (11–12) (2003) 1277–1304.

[5] L. Librescu, L. Meirovitch, S.S. Na, Control of cantilevers vibration via structural tailoring and adaptive materials, *AIAA Journal* 35 (8) (1997) 1309–1315.

[6] P.M. Naghdi, R.M. Cooper, Propagation of elastic waves in cylindrical shells, including the effects of transverse shear and rotatory inertia, *The Journal of the Acoustical Society of America* 28 (1) (1956) 56–63.

[7] A.H. Nayfeh, *Wave Propagation in Layered Anisotropic Media*, Elsevier, Amsterdam, The Netherlands, 1995, pp. 71–72.

[8] A.N. Palazotto, P.E. Linnemann, Vibration and buckling characteristics of composite cylindrical panels incorporating the effects of a higher order shear theory, *International Journal of Solids and Structures* 28 (3) (1991) 341–361.